6

HIGH-THROUGHPUT IDENTIFICATION OF ANTIGEN-SPECIFIC TCRS BY TCR GENE CAPTURE

Carsten Linnemann[1], Bianca Heemskerk[1,13], Pia Kvistborg[1,13], Roelof J.C. Kluin[2], Dmitriy A. Bolotin[3], Xiaojing Chen[4,5], Kaspar Bresser[1], Marja Nieuwland[2], Remko Schotte[1,6], Samira Michels[1], Raquel Gomez-Eerland[1], Lorenz Jahn[7], Pleun Hombrink[7], Nicolas Legrand[6,8,11], Chengyi Jenny Shu[1], Ilgar Z. Mamedov[3], Arno Velds[2], Christian U. Blank[1], John B.A.G. Haanen[1], Maria A. Turchaninova[3], Ron M. Kerkhoven[2], Hergen Spits[6,8,9], Sine Reker Hadrup[10], Mirjam H.M. Heemskerk[7], Thomas Blankenstein[4,5], Dmitriy M. Chudakov[3], Gavin M. Bendle[1,12,13] and Ton N.M. Schumacher[1,13]

[1]Division of Immunology and [2]Central Genomics Facility, The Netherlands Cancer Institute, Amsterdam, The Netherlands.
[3]Shemyakin-Ovchinnikov Institute of Bioorganic Chemistry RAS, Moscow, Russia.
[4]Max-Delbrück-Center for Molecular Medicine, Berlin, Germany.
[5]Institute of Immunology, Charité Campus Benjamin Franklin, Berlin, Germany.
[6]Department of Cell Biology and Histology, Academic Medical Center of the University of Amsterdam (AMC-UvA), Center for Immunology Amsterdam (CIA), Amsterdam, The Netherlands.
[7]Laboratory of Experimental Hematology, Department of Hematology, Leiden University Medical Center, Leiden, The Netherlands.
[8]AIMM Therapeutics, Amsterdam, The Netherlands.
[9]Tytgat Institute for Liver and Intestinal Research, Academic Medical Center of the University of Amsterdam (AMC-UvA), Amsterdam, The Netherlands.
[10]Center for Cancer Immune Therapy (CCIT), Herlev Hospital, Copenhagen, Denmark.
[11]Current address: AXENIS, Institut Pasteur, Paris, France.
[12]Current address: School of Cancer Sciences, University of Birmingham, Birmingham, UK.
[13]B.H and P.K, and T.N.M.S and G.M.B contributed equally.

Nature Medicine (In press)

The transfer of T-cell receptor (TCR) genes into patient T-cells is a promising approach for the treatment of both viral infections and cancer. While efficient methods exist to identify antibodies for the treatment of these diseases, comparable strategies for TCRs have been lacking. We have developed a high-throughput DNA-based strategy to identify TCR sequences, by the capture and sequencing of genomic DNA fragments encoding the TCR genes. We establish the value of this approach by the assembly of a large library of Cancer/Germline tumor-antigen reactive TCRs. Furthermore, exploiting the quantitative nature of TCR gene capture, we show the feasibility of identifying antigen-specific TCRs in oligoclonal T-cell populations, from either human material or TCR-humanized mice. Finally, we demonstrate the ability to identify tumor-reactive TCRs within intratumoral T-cell subsets without knowledge of antigen-specificities, forming the first step towards the development of autologous TCR gene therapy to target patient-specific neo-antigens in human cancer.

| INTRODUCTION

The treatment of cancer with T-cell-based therapies has seen major advances over the past decade[1]. These newly developed T-cell based immunotherapies either involve the administration of autologous tumor-reactive T-cell products that have been expanded *in vitro*[2,3], or infusion of *de novo* generated tumor-reactive T-cell populations, produced by introduction of tumor-reactive TCR genes into patient-derived T-cells. An attractive aspect of the former approach is that it exploits T-cell reactivity against both shared and patient-specific antigens. Attractive aspects of the latter approach – referred to as TCR gene therapy – are that it does not rely on pre-existing tumor-reactivity and allows the use of a set of highly tumor-reactive TCR genes for the treatment of larger patient groups[4,5].

Recent clinical studies of TCR gene therapy have provided the first evidence that this therapeutic approach can lead to cancer regression[6-8], and in particular the targeting of NY-ESO-1, one of the large group of Cancer/Germline (C/G) antigens, has shown clear clinical effects without demonstrable toxicity[8]. However, the NY-ESO-1 antigen is only expressed in a small fraction of human malignancies[8]. Likewise, expression of the other C/G-antigens is also only seen in a subset of patients[9,10], thereby making it essential to generate a large library of C/G antigen-reactive TCRs. Furthermore, it will be essential to develop such a tumor-reactive TCR library for many different HLA alleles. Because of this, the development of a strategy to rapidly identify TCRs of potential clinical interest – a possibility that readily exists for mAbs[11-13] – is of substantial interest.

| RESULTS

Development and validation of a TCR gene capture approach

In order to rapidly identify TCR sequences from large collections of samples, including clinical material, we sought to develop a DNA-based approach in which the genomic loci that encode the variable TCR sequences are captured and sequenced. To this purpose, we designed a bait library that targets each individual Variable (V)- and Joining (J)-element within the TCR α- and β-loci. This allows the selective isolation of the TCR-encoding genome elements from sheared (500 bp) genomic DNA (gDNA) fragments for subsequent paired-end deep sequencing (**Fig. 1a**). Furthermore, by indexing the genomic DNA of different T-cell samples, a highly multiplexed analysis of samples is feasible.

To first validate this method, we analyzed two CD8$^+$ T-cell clones, specific for the CMV pp65 antigen and minor-histocompatibility antigen HA-2, for which TCR αβ sequences had previously been determined[14]. We reasoned that analysis of resulting sequence data (approx. 500,000 on-target reads) could be achieved through two strategies. First, since TCR rearrangement involves the excision of large regions of genomic DNA, the mapping of sequence pairs to a reference genome should allow the one-step identification of DNA fragments that encompass the rearrangement site. Specifically, by *in silico* selection of those sequence pairs that are separated by a long distance (>1000 bp) within the parental genome, long range (TCR) rearrangements can be identified, and display of such sequence pairs in circular representations of the TCR loci provides a direct overview of functional and non-functional rearrangements within each T-cell population (**Supplementary Fig. 1a**). Second, we interrogated the same sequence data with an approach[15,16] that identifies Complementarity determining region 3 (CDR3) sequences on the basis of conserved Cysteine and Phenylalanine residues in TCR V- and J-elements.

Analysis of paired-end sequencing data from the CMV pp65 and HA-2 specific T-cell samples revealed the correct TCRαβ rearrangements by both strategies (shown for the CMV pp65 T-cell sample

Figure 1. Rapid assembly of a Cancer/Germline (C/G)-antigen specific TCR library by TCR gene capture. (**a**) Overview of the TCR gene capture process. Genomic DNA (gDNA) from multiple T-cell samples is sheared into 500 base-pair (bp) fragments and indexed for multiplexed TCR gene capture using a RNA-bait library specific for the TCR gene loci. Enriched DNA fragments are subjected to paired-end (75–100 bp) Illumina sequencing. TCR V(D)J rearrangements and CDR3 sequences are identified in the resulting sequence data. (**b**) Circular plots representing TCRα and TCRβ loci rearrangements identified in gDNA from SSX-2$_{KAS}$, MAGE-A2$_{YLQ}$, MAGE-C2$_{ALK}$ and NY-ESO-1$_{SLL}$ specific T-cells. Representative plots out of 42 samples analyzed are shown. Blue lines represent chromosomal positions of TCR V-elements and red lines mark TCR J-elements. Chromosomal rearrangements identified by mapping of paired-end reads are depicted by the lines connecting V- and J-elements. (**c**) pMHC-multimer stains of live, CD8$^+$ T-cells 13-16 days after retroviral transduction of primary human peripheral blood lymphocytes (PBLs) with indicated TCRs. The NY-ESO-1$_{SLL}$ TCR was tested against the high affinity variant peptide SLLMWITQ-C165A in Panel (c) and (d). (**d**) IFN-γ production of TCR-transduced (Td) PBLs in response to peptide-loaded target cells 13–16 days after retroviral transduction. Data were normalized by correction of the percentage IFN-γ$^+$ CD8$^+$ T-cells with the percentage of TCR Td CD8$^+$ T-cells. Please note that chromosomal rearrangements only occurring with low frequency are not displayed in the circular plots for reasons of clarity. ►

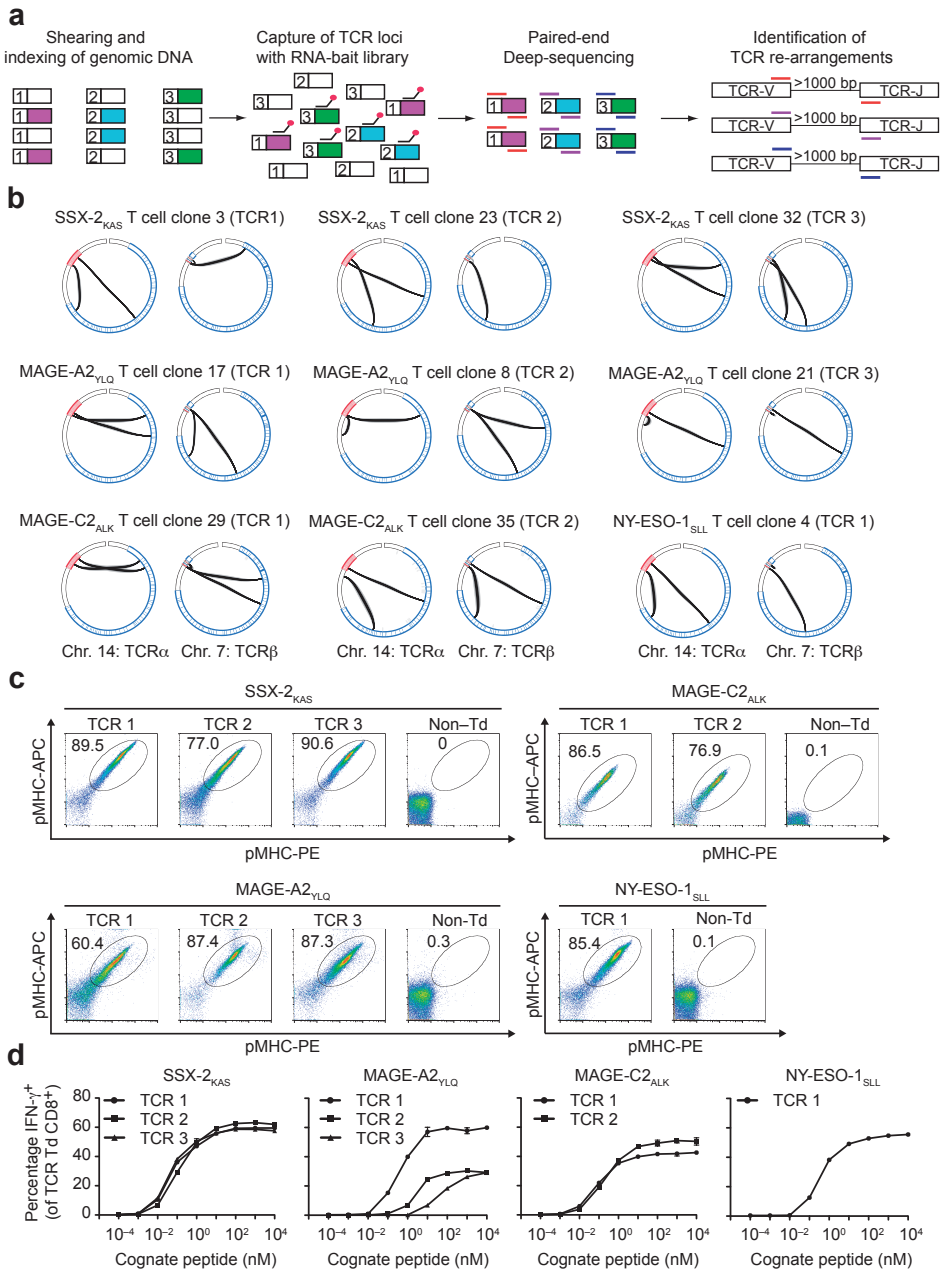
a
Shearing and indexing of genomic DNA
Capture of TCR loci with RNA-bait library
Paired-end Deep-sequencing
Identification of TCR re-arrangements
TCR-V
>1000 bp
TCR-J
b
SSX-2KAS T cell clone 3 (TCR1)
SSX-2KAS T cell clone 23 (TCR 2)
SSX-2KAS T cell clone 32 (TCR 3)
MAGE-A2YLQ T cell clone 17 (TCR 1)
MAGE-A2YLQ T cell clone 8 (TCR 2)
MAGE-A2YLQ T cell clone 21 (TCR 3)
MAGE-C2ALK T cell clone 29 (TCR 1)
MAGE-C2ALK T cell clone 35 (TCR 2)
NY-ESO-1SLL T cell clone 4 (TCR 1)
Chr. 14: TCRα
Chr. 7: TCRβ
c
SSX-2KAS
MAGE-C2ALK
MAGE-A2YLQ
NY-ESO-1SLL
TCR 1
TCR 2
TCR 3
Non–Td
Non-Td
89.5
77.0
90.6
0
86.5
76.9
0.1
60.4
87.4
87.3
0.3
85.4
0.1
pMHC-APC
pMHC-PE
d
SSX-2KAS
MAGE-A2YLQ
MAGE-C2ALK
NY-ESO-1SLL
Percentage IFN-γ+ (of TCR Td CD8+)
Cognate peptide (nM)

in **Supplementary Fig. 1a**). Furthermore, TCR identification was reliably successful with cell numbers as low as 500 T-cells (**Supplementary Fig. 1b**). At lower cell numbers, Illumina library preparation became less reliable, a limitation that may be overcome in the near future. More importantly, sorted single CD8$^+$ T-cells from both peripheral blood and tumor-infiltrating lymphocyte (TIL) material can be expanded to readily sufficient cell numbers (**Supplementary Fig. 1c**) in less than 2 weeks.

Assembly of a Cancer/Germline antigen-reactive TCR library

Having validated the TCR gene capture approach, we first utilized it to assemble a library of TCRs that may be used for TCR gene therapy of different human malignancies. To this purpose, peripheral blood or TIL samples from metastatic melanoma patients were analyzed by staining with a large collection of peptide-Major histocompatibility complex (pMHC)-multimers containing different tumor-associated peptides, to determine the presence of tumor-reactive T-cells[17,18]. This led to the identification of in total 147 T-cell responses against tumor-associated epitopes in samples from 61 patients, including one or multiple C/G-epitopes from HERV-K-MEL, LAGE-1, MAGE-A1, MAGE-A2, MAGE-A10, MAGE-C2, NY-ESO-1, SSX-2 and TAG (**Supplementary Fig. 2a** and data not shown). For each antigen of interest, single CD8$^+$, pMHC-multimer$^+$ T-cells were subsequently sorted and expanded. Resulting T-cell populations were validated by pMHC-multimer staining (**Supplementary Fig. 2b,c**) and then used for TCR capture.

Analysis of this large panel of defined antigen-specific T-cell populations led to the identification of 21 different TCRs against 11 different C/G-epitopes (**Fig. 1b**; **Supplementary Fig 3a**; **Table 1**) and three other tumor antigens (NA17A, MELOE-1, STEAP-1; data not shown). Importantly, the success rate for TCR identification from the clonal pMHC-multimer$^+$ T-cell populations that were analyzed was 100% (n = 113).

In order to validate the specificity of these TCRs, we retrovirally transduced primary human peripheral lymphocytes (PBLs). In all cases tested (n = 14), TCR-transduced CD8$^+$ T-cells stained positive with pMHC-multimers loaded with cognate peptide (**Fig. 1c** and **Supplementary Fig. 3b**). Furthermore, TCR gene transfer conferred the expected antigen reactivity against peptide-loaded targets, as shown by IFN-γ

Figure 2. TCR gene capture allows TCR identification in bulk antigen-specific T-cell populations obtained from clinical material by frequency-based matching. Circular plots representing the chromosomal rearrangements identified in gDNA from TAG_{RLS}, $MAGE\text{-}A1_{RVR}$ and $LAGE\text{-}1_{MLM}$ specific CD8$^+$ T-cells analyzed either (**a**) 14 days after single cell-sorting and subsequent expansion or (**b**) directly from bulk-sorted antigen-specific CD8$^+$ T-cells. (**c**) Frequency-based matching of clonotypic TCRαβ CDR3 sequences identified in sequence data of bulk-sorted antigen-specific T-cells. (**d**) Comparison of the relative frequency of TCRβ CDR3 sequences among sequenced T-cell clones and the corresponding bulk T-cell populations. (**e,g**) Circular plots representing the chromosomal rearrangements identified in gDNA isolated from bulk-sorted (**e**) $MAGE\text{-}A10_{GLY}$ CD8$^+$ T-cells from a T-cell line and (**g**) $Meloe\text{-}1_{TLN}$ specific CD8$^+$ T-cells from cultured TIL and frequency-based matching of clonotypic TCRαβ CDR3 sequences. (**f,h**) IFN-γ production of TCR Td PBLs in response to peptide-loaded target cells 12–14 days after retroviral transduction. Data were normalized by correction of the percentage IFN-γ$^+$ CD8$^+$ T-cells with the percentage of TCR Td CD8$^+$ T-cells. Please note that chromosomal rearrangements only occurring with low frequency are not displayed in the circular plots for reasons of clarity. ►

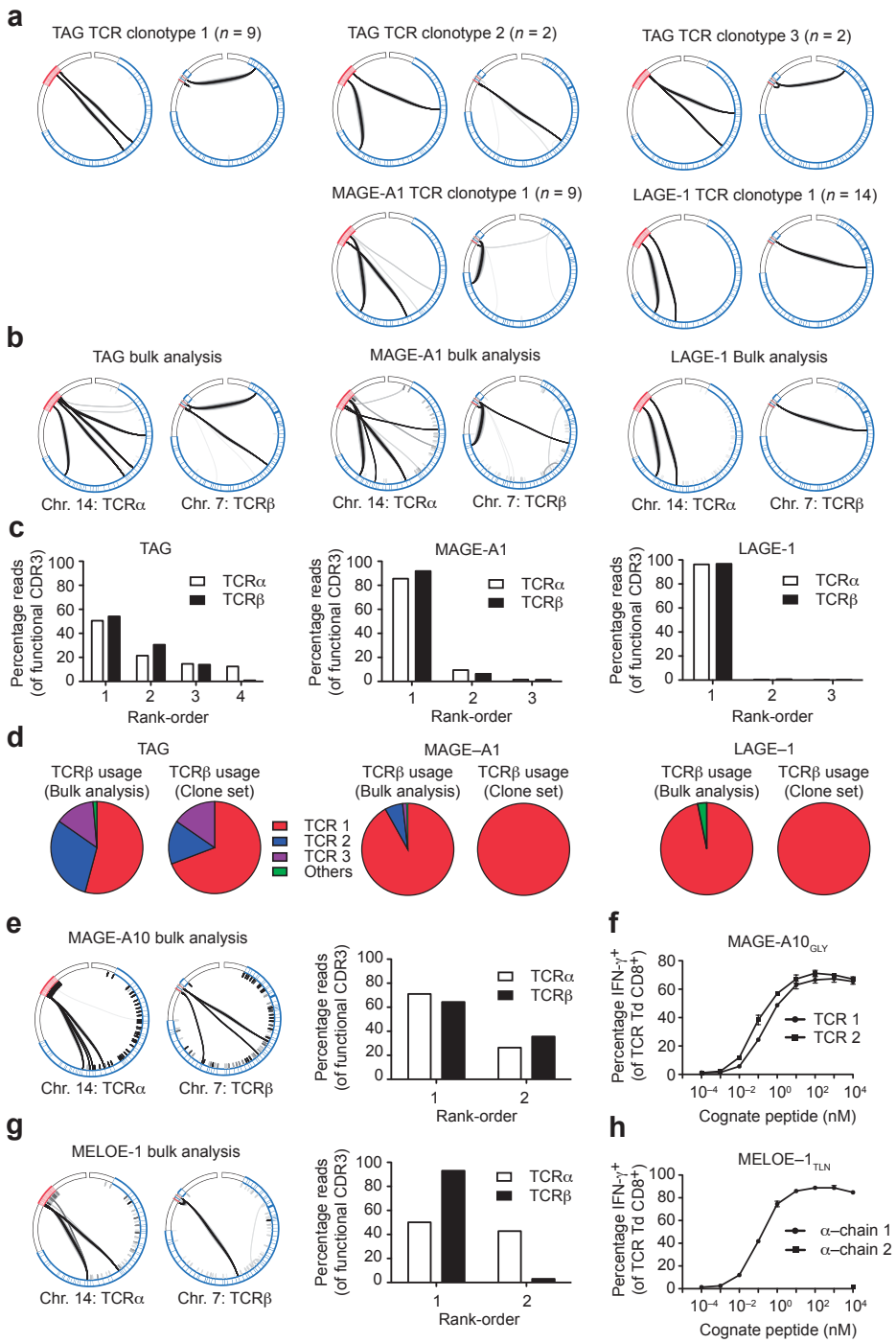
a
TAG TCR clonotype 1 (n = 9)
TAG TCR clonotype 2 (n = 2)
TAG TCR clonotype 3 (n = 2)
MAGE-A1 TCR clonotype 1 (n = 9)
LAGE-1 TCR clonotype 1 (n = 14)
b
TAG bulk analysis
MAGE-A1 bulk analysis
LAGE-1 Bulk analysis
Chr. 14: TCRα
Chr. 7: TCRβ
c
TAG
MAGE-A1
LAGE-1
Percentage reads (of functional CDR3)
TCRα
TCRβ
Rank-order
d
TAG
MAGE–A1
LAGE–1
TCRβ usage (Bulk analysis)
TCRβ usage (Clone set)
TCR 1
TCR 2
TCR 3
Others
e
MAGE-A10 bulk analysis
f
MAGE-A10GLY
Percentage IFN-γ+ (of TCR Td CD8+)
Cognate peptide (nM)
g
MELOE-1 bulk analysis
h
MELOE–1TLN
α–chain 1
α–chain 2

production (**Fig. 1d** and **Supplementary Fig. 3c**). Antigen-reactivity of these TCRs was further evaluated by assessing recognition of cell lines engineered to express cognate target antigen. For six out of seven epitopes analyzed, one or multiple TCRs showed recognition of endogenously expressed antigen, and for four epitopes recognition of tumor lines of different histologies was demonstrated (**Supplementary Fig. 4**). Of the 14 TCRs assessed, one (MAGE-$C2_{KVL}$ TCR 3) displayed non-specific reactivity (data not shown). Interestingly, some TCRs showed substantial pMHC-multimer binding but little or no recognition of tumor cells emphasizing the need to screen large sets of TCRs to select suitable TCRs for TCR gene therapy. Taken together, these data demonstrate that TCR gene capture is a highly efficient tool for the high-throughput assembly of TCR libraries from antigen-specific T-cell samples.

Analysis of antigen-specific TCR repertoires

The above experiments indicated that the heterogeneity of the TCR repertoire was in all instances quite limited, with only 1–3 TCRs being identified for each antigen-specific T-cell population (**Table 1**). As TCR gene capture provides quantitative data on the abundance of different TCR rearrangements, we speculated that it could be used to identify correct pairs of TCRαβ chains within a bulk sample of interest, by analyzing the data for TCRαβ CDR3 sequences that occur at the same frequency (i.e. 'frequency-based matching').

To examine the feasibility of such frequency-based matching, we obtained bulk T-cell populations specific for TAG_{RLS}, $LAGE\text{-}1_{MLM}$ and $MAGE\text{-}A1_{RVR}$ from TIL, as well as bulk CMV $pp65_{NLV}$-specific T-cells from a CMV-positive individual, by pMHC-multimer-based sorting (**Supplementary Fig. 5a** and data not shown). In parallel, single $CD8^+$ pMHC-$multimer^+$ T-cells were isolated from the same samples and expanded *in vitro*. We then rank-ordered the TCRα and TCRβ sequences identified within the bulk T-cell populations according to their relative frequency among functional CDR3s. For all four epitopes, the TCR clonotypes identified by frequency-based matching were identical to the ones found by single-cell analyses (**Fig. 2a–c** and **Supplementary Fig. 6a–c**). In addition, the reactivity of the two most abundant TCRαβ pairs identified within bulk CMV $pp65_{NLV}$ reactive T-cells was also confirmed by TCR gene transfer experiments (**Supplementary Fig. 6d,e**). Furthermore, the TCR clonotypes identified in these bulk samples generally comprised >95% of all identified functional CDR3s, and there was a close match between the abundance of the TCRβ CDR3 reads within bulk populations and the relative abundance of these TCRβ CDR3s among single-cell clones (**Fig. 2d** and **Supplementary Fig. 6f**).

Having validated this approach, two additional antigen-specific T-cell populations, specific for the C/G-antigen MAGE-A10 and the melanocyte-associated antigen MELOE-1, were analyzed without the parallel generation of clone sets (**Supplementary Fig. 5a**). This resulted in the identification of two $MAGE\text{-}A10_{GLY}$ specific TCR clonotypes (**Fig. 2e**) – reproducibly successful at different cell numbers (**Supplementary Fig. 7**) – that were both validated by TCR gene transfer (**Fig. 2f** and **Supplementary Fig. 5b**). The $MELOE\text{-}1_{TLN}$ specific T-cell population harbored a dominant TCRβ CDR3 (93%

Table 1. Library of Cancer/Germline antigen-specific TCRs identified with TCR gene capture.

Antigen	Epitope	HLA	Source	# seq. clones	# TCRs	TCR-Id	IC50 [nm]	TCR gene usage
HERV-Kmel	MLAVISCAV	A2	TIL (NKIR21)	12	2	1	n.d.	TRAV17 – TRAJ28; TRBV12 – TRBJ1-5
						2	n.d.	TRAV20 – TRAJ30; TRBV9 – TRBJ2-1
LAGE-1	MLMAQEALAFL	A2	TIL (NKIR21)	14	1	1	n.d.	TRAV36/DV7 – TRAJ43; TRBV10-1 – TRBJ2-1
MAGE-A1	RVRFFFPSL	B7	TIL (NKIRE01)	11	1	1	n.d.	TRAV35 – TRAJ26; TRBV27 – TRBJ2-1
MAGE-A2	YLQLVFGIEV	A2	PBMC (NKI-I04)	20	3	1	0.5	TRAV5 – TRAJ53; TRBV7-9 – TRBJ2-7
						2	3.4	TRAV5 – TRAJ53; TRBV7-9 – TRBJ2-7
						3	132.9	TRAV12-2 – TRAJ44; TRBV5-4 – TRBJ2-7
MAGE-A10	GLYDGMEHL	A2	TIL (NKIR06)	5	1	1	0.5	TRAV27 – TRAJ53; TRBV5-4 – TRBJ2-1
MAGE-C2	ALKDVEERV	A2	PBMC (NKI-I02)	5	2	1	0.7	TRAV5 – TRAJ1; TRBV6-5 – TRBJ1-2
						2	1.8	TRAV12-2 – TRAJ49; TRBV6-5 – TRBJ2-7
MAGE-C2	LLFGLALIEV	A2	TIL (NKIR06)	1	1	1	0.7	TRAV12-2 – TRAJ9; TRBV4-1 – TRBJ1-3
MAGE-C2	KVLEFLAKL	A2	PBMC (NKI-I01)	4	3	1	23.8	TRAV14/DV4 – TRAJ38; TRBV5-6 – TRBJ1-1
						2	12.1	TRAV38-1– TRAJ57; TRBV13 – TRBJ2-5
						3	35.3	TRAV12-2 – TRAJ49; TRBV6-5 – TRBJ1-2
NY-ESO-1	SLLMWITQC	A2	PBMC (NKI-I05)	10	1	1	1.6	TRAV17– TRAJ27; TRBV12-4– TRBJ1-1
SSX-2	KASEKIFYV	A2	PBMC (NKI-I03)	7	3	1	0.05	TRAV38-2/DV8– TRAJ54; TRBV3-1 – TRBJ1-4
						2	0.1	TRAV12-2 – TRAJ47; TRBV19 – TRBJ1-5
						3	0.03	TRAV5 – TRAJ34; TRBV20-1 – TRBJ2-1
TAG	RLSNRLLLR	A3	TIL (NKIRE02)	12	3	1	n.d.	TRAV12-3 – TRAJ6; TRBV5-1 – TRBJ2-1
						2	n.d.	TRAV12-1 – TRAJ13; TRBV5-5 – TRBJ1-3
						3	n.d.	TRAV12-3 – TRAJ6; TRBV5-1 – TRBJ2-1

of functional CDR3 reads) and two TCRα CDR3s that were both detected at a comparable frequency (50% and 43% of functional CDR3 reads, respectively; **Fig. 2g**). Analysis of T cells modified with either TCRαβ pair demonstrated that only T-cells that were transduced with TCR α-chain 1 displayed MELOE-1 reactivity (**Fig. 2h** and **Supplementary Fig. 5c**), suggesting that this T-cell population was largely comprised of a single T-cell clone with two functional TCRα rearrangements. Collectively, these data demonstrate that TCR gene capture can be used to unravel the composition of TCR repertoires and correctly reconstruct TCRαβ pairs in six out of six bulk populations of antigen-specific T-cells tested.

While human cancer patients, and in particular melanoma patients frequently display T-cell reactivity against a number of tumor-associated antigens, it has been argued that for many of the encoded TCRs affinity for pMHC may be suboptimal, as a consequence of thymic or peripheral deletion[19]. To circumvent this issue, a number of platforms have been developed that allow the induction or selection of T-cells that have not been subjected to thymic tolerance for the pMHC of interest[20-24]. To test the potential of TCR gene capture to obtain TCRs against antigens of interest from these platforms, we performed captures from T-cell samples obtained from HLA-mismatched individuals[20,21,25], from immunodeficient mice reconstituted with human hematopoietic progenitors[26,27] and from mice transgenic for the human TCR α- and β-loci[23].

First, allo-HLA-restricted CD8$^+$ T-cell populations specific for two HLA-A2 restricted CD79b lineage antigen epitopes were obtained by pMHC-multimer based enrichment of PBLs from an HLA-A2 negative individual[28]. TCR capture analysis of these CD8$^+$ T-cell populations revealed two different TCRs against the epitopes within this antigen (**Supplementary Fig. 8** and M.H.M. Heemskerk, manuscript in preparation). Second, Balb/c *Rag2*$^{-/-}$ *Il2rg*$^{-/-}$ mice were reconstituted with human hematopoietic progenitor cells that had been lentivirally modified with a MART-1 specific TCRβ chain[29] to skew the resulting TCR repertoire towards MART-1 reactivity. Analysis of short-term expanded MART-1 pMHC-multimer$^+$ CD8$^+$ T-cell clones obtained from these mice revealed a series of non-native TCRα chains (**Supplementary Fig. 9a**). Further analysis of two of these by TCR gene transfer into human PBL together with the original TCRβ chain showed they displayed the anticipated MART-1 antigen reactivity (**Supplementary Fig. 9b,c**). Finally, we set out to identify TCRs from HLA-A2 transgenic mice that have been rendered transgenic for the human TCRα- and β-loci[23]. To this purpose, bulk CD8$^+$ T-cell populations specific for NY-ESO-1$_{SLL}$ peptide (**Fig. 3a**) were isolated from vaccinated mice and analyzed by TCR gene capture. As was observed for many human antigen-specific CD8$^+$ T-cell populations (**Fig. 2**), the NY-ESO-1$_{SLL}$-specific T-cell responses in human TCR mice were mainly dominated by one TCR clonotype (**Fig. 3b,c**). Importantly, identified dominant TCRαβ pairs conferred NY-ESO-1 antigen reactivity to human PBLs, as shown by pMHC-multimer staining (**Fig. 3d**) and functional activity against peptide-loaded targets (**Fig. 3e**). In addition, a second functional TCRαβ pair was identified for mouse 1, by combination of the second-

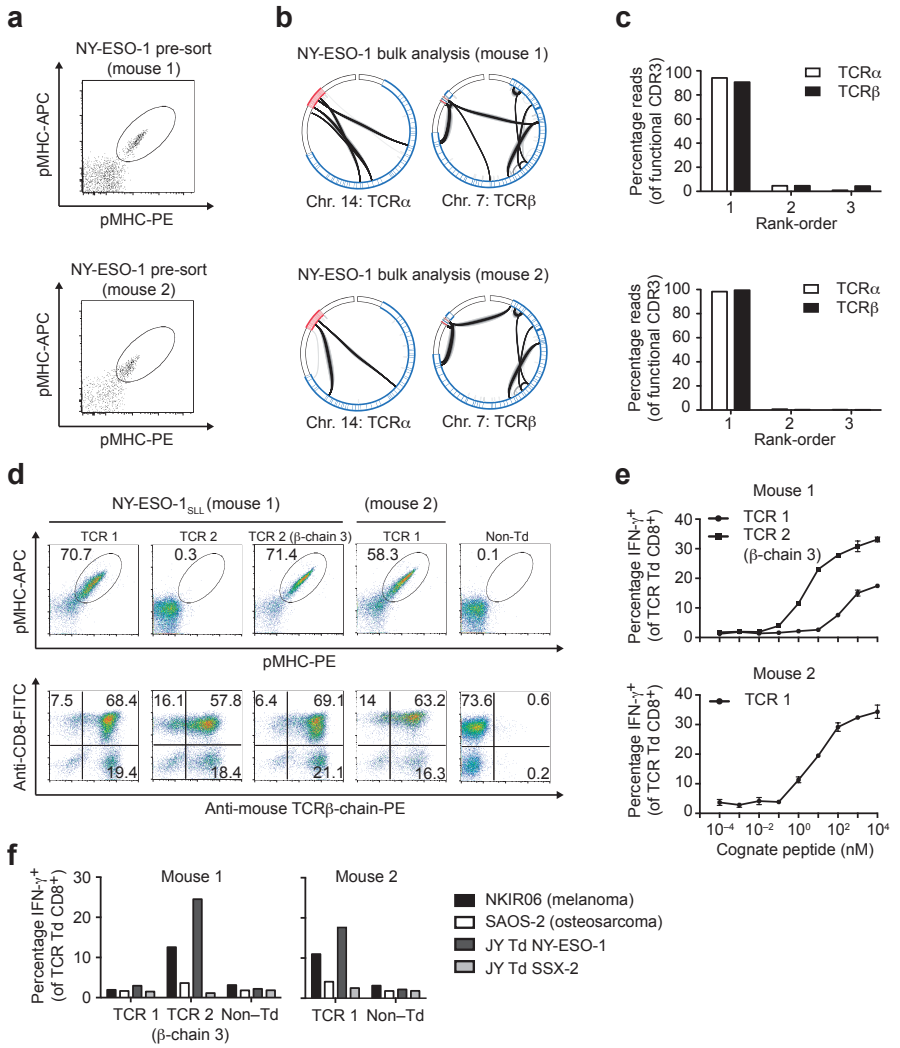

Figure 3. Identification of NY-ESO-1 specific TCRs in antigen-specific T-cell populations from mice with a diverse human TCR repertoire. (**a**) pMHC-multimer staining of live, CD8$^+$ T-cells in peripheral blood of individual mice 6 days after NY-ESO-1$_{SLL}$ peptide booster-vaccination. (**b**) Circular plots representing the chromosomal rearrangements identified in gDNA isolated from bulk-sorted NY-ESO-1$_{SLL}$-specific CD8$^+$ T-cells from hTCR transgenic AaBbDII mice. (**c**) Frequency-based matching of clonotypic TCRαβ CDR3 sequences within the sequence data of bulk-sorted NY-ESO-1$_{SLL}$-specific CD8$^+$ T-cells from AaBbDII mice. (**d**) pMHC-multimer staining of live, CD8$^+$ T-cells 7 days after retroviral transduction of primary human PBLs. (**e**) IFN-γ production of TCR Td PBLs in response to peptide-loaded target cells 7 days after retroviral transduction of human PBLs Td with indicated NY-ESO-1$_{SLL}$-specific TCRs. Data were normalized by correction of the percentage IFN-γ$^+$ CD8$^+$ T-cells by the percentage of TCR Td CD8$^+$ T-cells. The NY-ESO-1$_{SLL}$ TCRs were tested against the high affinity variant peptide SLLMWITQ-C165A in (d) and (e). (**f**) IFN-γ production of TCR Td PBLs in response to various tumor cell lines and a control cell line expressing NY-ESO-1 antigen, analyzed 7 days after retroviral transduction. Data were normalized by correction of the percentage IFN-γ$^+$ CD8$^+$ T-cells with the percentage of TCR Td CD8$^+$ T-cells. Please note that chromosomal rearrangements only occurring with low frequency are not displayed in the circular plots for reasons of clarity.

ranked TCRα CDR3 with the third-ranked TCRβ CDR3 (note that the second- and third-ranked TCRβ were present at near identical frequencies, at 4.6% and 4.4% of functional TCRβ CDR3s) (**Fig. 3d,e**). For two out of three identified TCRs, functional activity towards NY-ESO-1 expressing tumor cells could also be observed (**Fig. 3f**).

Dissecting intratumoral tumor-reactive TCR repertoires

In the above experiments, prior knowledge of antigen-reactivity was used to obtain T-cell populations for TCR capture. While TCRs specific for such known shared antigens are conceptually attractive for TCR gene therapy (i.e. applicable for larger patient groups), there is an increasing interest in targeting patient-specific neo-antigens, in particular for tumor types such as melanoma and NSCLC in which mutational loads are high[30,31].

To test whether a library of tumor-reactive TCRs can be generated for individual patients without prior knowledge of antigen-specificity, we generated a panel of short-term expanded $CD8^+$ T-cell populations from single $CD8^+$ T-cells recovered from a metastatic melanoma. Subsequently, tumor-reactivity of these T-cell populations was determined by analysis of CD107a (LAMP-1) and CD137 (4-1BB) expression upon culture with autologous tumor (**Supplementary Fig. 10a**). 15% of the T-cell populations analyzed (34/234) exhibited clear recognition of autologous tumor, and TCRs in 31 of these T-cell populations were characterized by TCR gene capture (**Supplementary Fig. 10a**). This analysis revealed 19 different tumor-reactive TCRs (**Supplementary Fig. 10b,c**), demonstrating both that the tumor-reactive TCR repertoire can be broad, and that it is feasible to rapidly assemble a library of patient-specific tumor-reactive TCRs by TCR gene capture.

To assess whether tumor-reactive TCRs can also be identified in bulk $CD8^+$ T-cell populations in melanoma, we isolated tumor-reactive, $CD8^+$ T-cells among TIL after co-culture with autologous tumor by $CD107a^+$ staining (**Fig. 4a**). Analysis of the $CD107a^+$ T-cell subset by TCR gene capture showed a diverse TCR repertoire (**Fig. 4b**). Nevertheless, the most dominant TCR (comprising approx. 15% of total functional CDR3s, **Fig. 4c**) was identical to a TCR clonotype that had also been identified from tumor-reactive single sorted $CD8^+$ cells from this subject (**Supplementary Fig. 10c**; TCR

Figure 4. Unbiased identification of tumor-reactive TCRs within oligoclonal intratumoral T cell populations. (**a**) Expression of CD107a on $CD8^+$ T-cells from TIL with or without prior stimulation with autologous tumor. (**b**) Circular plots representing the chromosomal rearrangements identified in gDNA isolated from bulk-sorted $CD8^+$ $CD107a^+$ T-cells from tumor-stimulated TIL. (**c**) Frequency-based matching of clonotypic TCRαβ CDR3 sequences identified in sequence data from bulk-sorted $CD8^+$ $CD107a^+$ T-cells from TIL. (**d**) IFN-γ production of TCR Td PBLs in response to autologous tumor cells analyzed 12 days after retroviral transduction. Data were normalized by correction of the percentage IFN-γ^+ $CD8^+$ T-cells by the percentage of TCR Td $CD8^+$ T-cells. (**e**) TCR Vβ gene usage in $CD107a^+CD8^+$ TIL after stimulation with autologous tumor cells. (**f**) Circular plots representing the TCRα and TCRβ loci rearrangements identified in gDNA isolated from indicated bulk-sorted $CD8^+$ $CD107a^+$ T-cell subsets with defined TCR Vβ gene usage after stimulation with autologous tumor cells. (**g**) Circular plots representing the TCR clonotypes identified in gDNA from selected short-term expanded cloned $CD8^+$ T-cells reactive against autologous tumor (as identified in **Supplementary Fig. 10**). (**h**) Frequency-based matching of clonotypic TCRαβ CDR3 sequences identified in sequence data from bulk-sorted $CD8^+$ $CD107a^+$ T-cells subsets with defined TCR Vβ gene usage. Please note that chromosomal rearrangements only occurring with low frequency are not displayed in the circular plots for reasons of clarity. ►

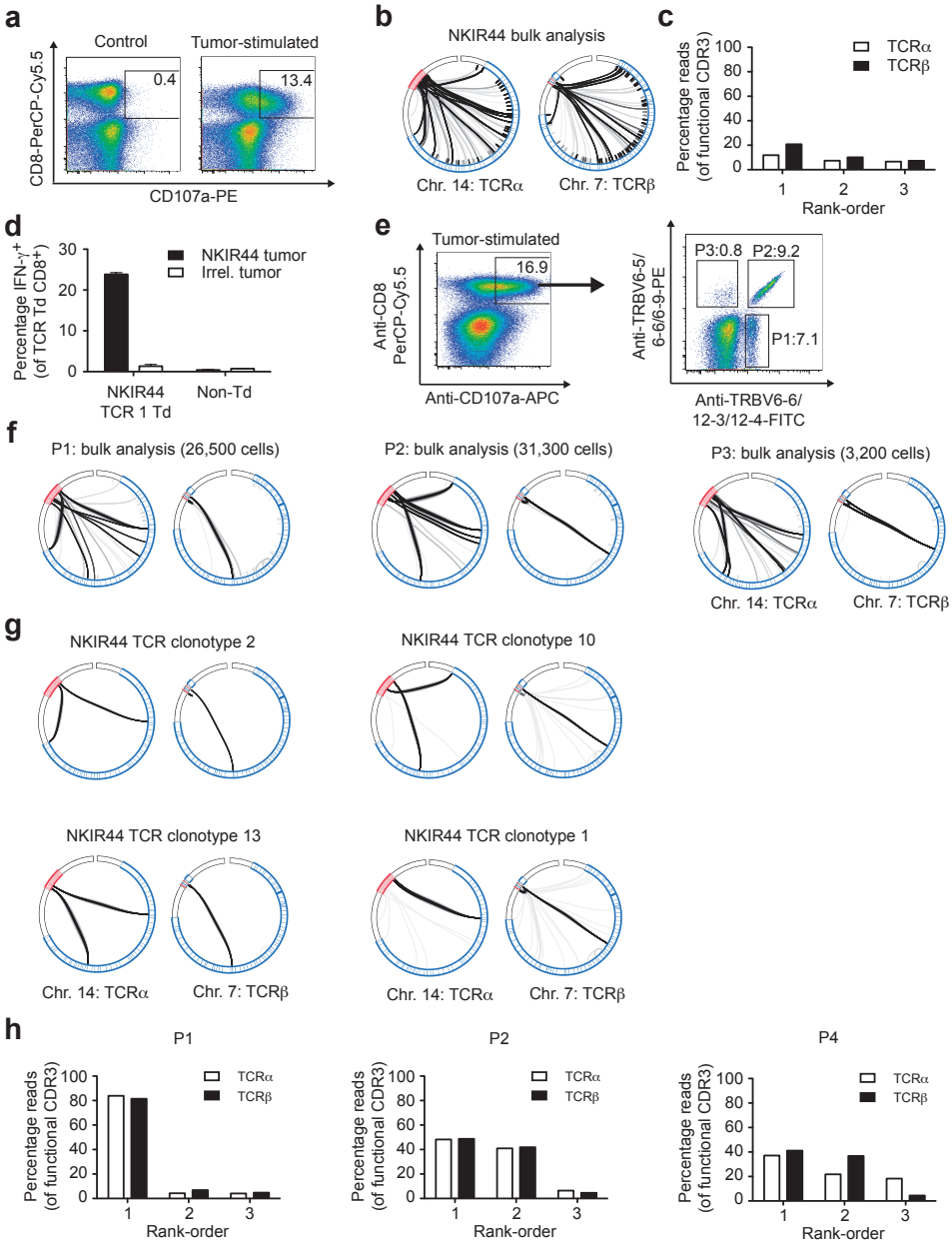
a
Control
Tumor-stimulated
CD8-PerCP-Cy5.5
0.4
13.4
CD107a-PE
b
NKIR44 bulk analysis
Chr. 14: TCRα
Chr. 7: TCRβ
c
Percentage reads (of functional CDR3)
TCRα
TCRβ
Rank-order
d
Percentage IFN-γ+ (of TCR Td CD8+)
NKIR44 tumor
Irrel. tumor
NKIR44 TCR 1 Td
Non-Td
e
Tumor-stimulated
16.9
Anti-CD8 PerCP-Cy5.5
Anti-CD107a-APC
P3:0.8
P2:9.2
P1:7.1
Anti-TRBV6-5/ 6-6/6-9-PE
Anti-TRBV6-6/ 12-3/12-4-FITC
f
P1: bulk analysis (26,500 cells)
P2: bulk analysis (31,300 cells)
P3: bulk analysis (3,200 cells)
Chr. 14: TCRα
Chr. 7: TCRβ
g
NKIR44 TCR clonotype 2
NKIR44 TCR clonotype 10
NKIR44 TCR clonotype 13
NKIR44 TCR clonotype 1
Chr. 14: TCRα
Chr. 7: TCRβ
h
P1
P2
P4
Percentage reads (of functional CDR3)
TCRα
TCRβ
Rank-order

5). Furthermore, TCR gene transfer into human PBL confirmed reactivity of this TCR against autologous tumor (**Fig. 4d**). In addition, while the frequency of all TCRs that were next in rank differed only minimally (< 1.5-fold), TCRαβ pair 2 was nevertheless identical to a previously determined TCR (**Supplementary Fig. 10c**; TCR 10).

In order to enhance the resolution of frequency-based matching, $CD8^+$ $CD107a^+$ T-cell populations were also analyzed following separation on the basis of TCR Vβ-usage (**Fig. 4e**). In these samples, strong dominance of 1–2 TCR clonotypes, comprising ≥ 80% of all functional CDR3s was observed, and for two out of three subsets (P1, P2), the correct ranking of the two most dominant TCRαβ pairs could directly be confirmed by comparison with the TCR clonotypes obtained from short-term expanded single cells (**Fig. 4f–h** and **Supplementary Fig. 10**). Taken together, these data demonstrate that TCR gene capture can be used to unravel the composition of TCR repertoires and correctly identify dominant tumor-reactive TCRαβ pairs within intratumoral T-cell subsets – even without knowledge of the antigen(s) involved.

| DISCUSSION

Here we describe TCR gene capture as a strategy to obtain TCR sequences from large numbers of samples and with a very high success rate. We have used this approach to 1. assemble a library of tumor-reactive TCRs from patient material and from different 'non-tolerant sources', 2. identify TCRαβ pairs in bulk antigen-specific T-cell populations in either human material or from humanized mice, and 3. assess the TCR repertoire of intratumoral T-cell subsets without knowledge of antigen specificity.

The approach that we have developed differs in a number of ways from RNA-based strategies that aim to describe TCR repertoires from single cells[32,33]. First, the approach described here is not performed on single cells but rather on bulk cells or on single cells that have been expanded for a short period of time. A potential concern is that short-term cell expansion would result in a bias towards certain TCR clonotypes. However, expansion of both peripheral blood cells and TIL (**Table 1**) to the low cell numbers required was shown to be reliable. Furthermore, comparison of the TCR repertoire obtained following this short-term expansion with that observed by bulk analysis (**Fig. 2**) directly demonstrated that if such a bias exists, at least for the material analyzed here it is minimal. Short-term expansion also allows one to confirm the antigen specificity or tumor-reactivity of each T-cell for which the TCR clonotype is described. We consider this a useful property, as re-analysis of expanded MHC multimer-sorted T-cells reveals the presence of false positives with a substantial frequency (10% or greater). This issue becomes particularly apparent when analyzing the very low magnitude T-cell responses we have successfully analyzed here. Because of its quantitative nature, TCR gene capture also allows the analysis of bulk T-cell populations without a need for single cell isolation. Such bulk analyses will be useful to describe TCR repertoires in T-cell subsets, such as regulatory T-cells that may be more difficult to expand, from either fresh or archived patient material.

We speculate that TCR gene capture will be valuable for two main purposes. First, it will allow one to describe the TCR repertoire in diverse types of biological samples, either by short-term expansion of T-cells or by bulk analysis. This makes it possible to describe (and recreate) the TCR repertoire at sites of, for instance, viral infection or autoimmune disease. Second, the technology will allow the creation of large collections of TCR genes for genetic engineering of T-cell immunity. With respect to the latter application, we demonstrate that our approach can be utilized to rapidly identify tumor-reactive TCR genes in a patient-specific manner, likely including TCR genes that are reactive to patient-specific neo-antigens[34-36]. If such TCRs can also be rapidly re-introduced into autologous T-cells, preferably in conjunction with a suicide switch[37,38], this would allow one to 'transplant' the tumor-reactive TCR repertoire from exhausted T-cells into a more fit T-cell population. While such autologous TCR gene therapy will not be achieved in the coming years, the observations that successful treatment of human malignancy can be achieved with low cell numbers[39] and that non-viral gene delivery is feasible[40] do suggest that such an approach may become a realistic goal.

| METHODS

RNA-bait library design. For TCR gene capture we designed a target enrichment library (Agilent) by identifying chromosomal locations of functional TCR V- and J-elements using the IMGT database (http://www.imgt.org) and targeting these with multiple, tiled 120 basepair (bp) RNA-baits. In this design, every TCR V-element is targeted by an average of eight different baits. TCR J-elements, which are significantly shorter than 120 bp, were extended into the non-coding region to accommodate on average six bait sequences. Full details on bait design are available upon request.

TCR gene capture. DNA was isolated from T-cell samples using the QIAamp DNA Micro kit, QIAamp DNA Mini kit or Blood&Tissue DNA isolation kit (Qiagen). In general, approximately 3 µg of DNA was sheared to 500–600 bp fragments with a Covaris system (S-series, D10%, I5, C/b 200, 30 s) and resulting DNA fragments were purified with SPRI beads (Agencourt). Sequence libraries were prepared using the TruSeq DNA library preparation kit (Illumina) with the adaptation of only seven cycles for the final library amplification. Illumina Truseq 6 bp indexes (as designed by the manufacturer) were introduced into each DNA library to allow multiplexing. For samples with a low DNA yield (< 100 ng), shearing conditions were adapted to maintain standard fragment lengths. Furthermore, we used a 1:10 diluted adapter concentration in the library preparation and performed four additional PCR cycles to obtain comparable library amounts.

Multiplexed TCR captures were performed using a custom-designed Agilent SureSelect bait library according to manufacturer's guidelines for Illumina Paired-End Sequencing Library (version 1.2) with the following adaptations. Pools of 6–8 DNA libraries were captured with 1/10 of a bait reaction. Furthermore, Block #3

in the hybridization mixture was replaced with a custom NKI-Block #3 to support the TruSeq DNA libraries in which the indexes require additional blocking. NKI-Block #3 consists of equal amounts of two DNA oligos (IDT-DNA, Iowa, US) at 16.6 μg μl^{-1}:

NKI 3.1
5'-AGATCGGAAGAGCACACGTCTGAA
CTCCAGTCACNNNNNNATCTCGTA
TGCCGTCTTCTGCTTG/3'ddC/ -3'
NKI 3.2
5'-CAAGCAGAAGACGGCATACGAGAT
NNNNNNGTGACTGGAGTTCAGAC
GTGTGCTCTTCCGATCT/3'ddC/ -3'

Captured library fragments were split into two fractions for PCR enrichment (15 cycles) using the Illumina P5 and P7 oligonucleotides (IDT-DNA, Iowa, US)

P5 primer: 5'-AATGATACGGCGACCACC
GAGATCT-3'
P7 primer:5'-CAAGCAGAAGACGGCAT
ACGAG-3'

Both PCR reactions were quantified on a BioAnalyzer DNA Chip (Agilent), combined in equal amounts and diluted to 10 nM concentrations. Subsequently, paired-end sequencing of samples was carried out with a read-length of 75–100 bp using the Illumina Hiseq2000 platform.

Analysis of Illumina sequence data. Sequencing reads in fastq files were mapped to the human genome, build NCBI36/hg18, using bwa[41] and samtools[42]. PCR duplicates in resulting bam files were filtered using Picard (http://picard.sourceforge.net). "Jumping" pairs that report on chromosomal (TCR) rearrangements were counted per 1000 bp within the TCR regions on chromosome 7 (141600 kb and 142300 kb) and chromosome 14 (21100 kb and 22200 kb). A pair was considered to be "jumping" if mapping qualities were greater than 36 and sequence pairs had an insert size greater than 1000 bp, as based on mapping to the reference genome. Circular plots were created using Circos[43] with the darkness of the links and broadness of the bezier curve range reflecting the number of "jumping" pairs.

CDR3 TCR sequences were identified as previously reported[15,16]. Briefly, we localized the TCR J-gene element in each sequence read based on the identity of a short six nucleotide-motif for every TCR J-gene (http://www.imgt.org) containing the conserved Phenylalanine. TCR J-gene identity was expanded in both directions until the last matched nucleotide was encountered. At least 12 aligned nucleotides were required as a minimum for the identification of TCR J-genes. Similarly, we identified the TCR V-gene element using the conserved Cysteine residue. TCRβ-D gene elements were localized based on the identity of at least six nucleotides between TCR V- and TCR J-gene elements. The CDR3 was extracted for each read as the nucleotide sequence between the conserved TCR V-segment Cysteine and TCR J-segment Phenylalanine residues. Extracted CDR3 with identical nucleotide sequences were clustered to clonotypes with PCR and sequencing error correction as described[16].

Retroviral vector for T-cell receptor expression. A modified pMP71-TCR-flex retroviral backbone for TCR cloning was generated by introducing unique cut-sites to rapidly exchange variable TCR domains (**Supplementary Fig. 11**). To maximize TCR expression, the vector contains codon-optimized murine TCRαβ constant domains with additional Cysteine residues and a porcine teschovirus-derived P2A sequence to link TCR chains. Variable TCRα- and β-fragments of identified TCRs were codon-

optimized, synthesized and cloned by Genscript, CRO. A detailed description of the retroviral transduction of human PBLs can be found in the Supplementary Methods.

| ACKNOWLEDGEMENTS

We are grateful to A. Pfauth, F. van Diepen and B. Hooibrink for assistance with flow cytometry and to M. Nagasawa, T. Heidebrecht, E. Siteur- van Rijnstra, K. Weijer, M. Böhne, M. van der Maas, W. van de Kasteele and T. de Jong for technical assistance. The Bloemenhove Clinic (Heemstede, The Netherlands) is acknowledged for providing fetal tissues. We thank A. Kaiser, S. Naik and J. Rohr for critical discussions.

C.L is a fellow in the PhD Fellowship Program of Boehringer Ingelheim Fonds-Foundation for Basic Research in Biomedicine. M.A.T, I.Z.M. D.A.B and D.M.C are supported by MCB program of the Russian Academy of Sciences, RFBR 12-04-33139 and 12-04-00229-a. G.M.B is the recipient of a Leukaemia and Lymphoma Research Bennett senior non-clinical Fellowship (12004). T.B is supported by the Deutsche Forschungsgemeinschaft through Sonderforschungsbereich TR36. This work was supported by grants from The Dutch Cancer Society (NKI 2009-4282 to T.N.M.S, J.B.A.G.H and G.M.B and NKI 2006-3530 to T.N.M.S and H.S) and The Danish Council for Strategic Research (09-065152 to S.R.H and T.N.M.S).

| AUTHOR CONTRIBUTIONS

C.L designed, performed, analyzed/interpreted all experiments and wrote the paper. B.H designed, performed, analyzed and interpreted experiments for the analysis of bulk antigen-specific T-cell responses and T-cell subsets in TIL and helped in designing, performing, analyzing and interpreting C/G-TCR validation experiments. P.K identified C/G-antigen specific T-cell responses and helped in designing, performing, analyzing and interpreting C/G-TCR validation experiments. R.J.C.K and A.V performed bioinformatic analysis to identify chromosomal rearrangements. X.C designed, performed, analyzed and interpreted experiments in AaBbDII mice. R.S, N.L and R.G.E designed, performed, analyzed and interpreted experiments with HIS-mice. L.J and P.H designed, performed, analyzed and interpreted experiments to raise allo-TCRs against CD79b. C.J.S. identified C/G-antigen specific T-cell responses in TIL, contributed to RNA bait library design and performed initial validations. K.B and S.M assisted in TCR validation experiments. M.N and R.M.K performed TCR gene capture, Illumina sequencing and analyzed/interpreted data. C.U.B and J.B.A.G.H provided patient material. M.A.T, I.Z.M, D.A.B and D.M.C, performed bioinformatic analysis to identify CDR3s and analyzed/interpreted data. H.S designed and interpreted experiments in HIS-mice. S.R.H identified C/G-antigen specific T-cell responses and provided patient material. M.H designed and interpreted experiments to raise allo-TCRs against CD79b T.B designed and interpreted experiments in AaBbDII mice. G.M.B co-supervised the project, designed, performed, analyzed/interpreted all experiments and wrote the paper. T.N.M.S developed the concept of TCR gene capture, supervised the project, designed and interpreted all experiments and wrote the paper.

| REFERENCES

1. Restifo, N.P., Dudley, M.E. & Rosenberg, S.A. Adoptive immunotherapy for cancer: harnessing the T cell response. *Nat Rev Immunol* **12**, 269-281 (2012).
2. Dudley, M.E., *et al.* Cancer regression and autoimmunity in patients after clonal repopulation with antitumor lymphocytes. *Science* **298**, 850-854 (2002).
3. Besser, M.J., *et al.* Clinical responses in a phase II study using adoptive transfer of short-term cultured tumor infiltration lymphocytes in metastatic melanoma patients. *Clin Cancer Res* **16**, 2646-2655 (2010).
4. Schumacher, T.N. T-cell-receptor gene therapy. *Nat Rev Immunol* **2**, 512-519 (2002).
5. Linnemann, C., Schumacher, T.N. & Bendle, G.M. T-cell receptor gene therapy: critical parameters for clinical success. *J Invest Dermatol* **131**, 1806-1816 (2011).
6. Morgan, R.A., *et al.* Cancer regression in patients after transfer of genetically engineered lymphocytes. *Science* **314**, 126-129 (2006).
7. Johnson, L.A., *et al.* Gene therapy with human and mouse T-cell receptors mediates cancer regression and targets normal tissues expressing cognate antigen. *Blood* **114**, 535-546 (2009).
8. Robbins, P.F., *et al.* Tumor regression in patients with metastatic synovial cell sarcoma and melanoma using genetically engineered lymphocytes reactive with NY-ESO-1. *J Clin Oncol* **29**, 917-924 (2011).
9. Simpson, A.J., Caballero, O.L., Jungbluth, A., Chen, Y.T. & Old, L.J. Cancer/testis antigens, gametogenesis and cancer. *Nat Rev Cancer* **5**, 615-625 (2005).
10. Scanlan, M.J., Simpson, A.J. & Old, L.J. The cancer/testis genes: review, standardization, and commentary. *Cancer Immun* **4**, 1 (2004).
11. Reddy, S.T., *et al.* Monoclonal antibodies isolated without screening by analyzing the variable-gene repertoire of plasma cells. *Nat Biotechnol* **28**, 965-969 (2010).
12. Kwakkenbos, M.J., *et al.* Generation of stable monoclonal antibody-producing B cell receptor-positive human memory B cells by genetic programming. *Nat Med* **16**, 123-128 (2010).
13. Wrammert, J., *et al.* Rapid cloning of high-affinity human monoclonal antibodies against influenza virus. *Nature* **453**, 667-671 (2008).
14. Heemskerk, M.H., *et al.* Efficiency of T-cell receptor expression in dual-specific T cells is controlled by the intrinsic qualities of the TCR chains within the TCR-CD3 complex. *Blood* **109**, 235-243 (2007).
15. Mamedov, I.Z., *et al.* Quantitative tracking of T cell clones after haematopoietic stem cell transplantation. *EMBO Mol Med* **3**, 201-207 (2011).
16. Bolotin, D.A., *et al.* Next generation sequencing for TCR repertoire profiling: Platform-specific features and correction algorithms. *Eur J Immunol* **42**, 3073-3083 (2012).
17. Andersen, R.S., *et al.* Dissection of T-cell antigen specificity in human melanoma. *Cancer Res* **72**, 1642-1650 (2012).
18. Kvistborg, P., *et al.* TIL therapy broadens the tumor-reactive CD8(+) T cell compartment in melanoma patients. *OncoImmunology* **1**, 409-418 (2012).
19. Derbinski, J. & Kyewski, B. How thymic antigen presenting cells sample the body's self-antigens. *Curr Opin Immunol* **22**, 592-600 (2010).
20. Sadovnikova, E. & Stauss, H.J. Peptide-specific cytotoxic T lymphocytes restricted by nonself major histocompatibility complex class I molecules: reagents for tumor immunotherapy. *Proc Natl Acad Sci U S A* **93**, 13114-13118 (1996).
21. Amir, A.L., *et al.* PRAME-specific Allo-HLA-restricted T cells with potent antitumor reactivity useful for therapeutic T-cell receptor gene transfer. *Clin Cancer Res* **17**, 5615-5625 (2011).
22. Li, Y., *et al.* Directed evolution of human T-cell receptors with picomolar affinities by phage display. *Nat Biotechnol* **23**, 349-354 (2005).
23. Li, L.P., *et al.* Transgenic mice with a diverse human T cell antigen receptor repertoire. *Nat Med* **16**, 1029-1034 (2010).
24. Stanislawski, T., *et al.* Circumventing tolerance to a human MDM2-derived tumor antigen by TCR gene transfer. *Nat Immunol* **2**, 962-970 (2001).
25. Wilde, S., *et al.* Dendritic cells pulsed with RNA encoding allogeneic MHC and antigen induce T cells with superior antitumor activity and higher TCR functional avidity. *Blood* **114**, 2131-2139 (2009).
26. Traggiai, E., *et al.* Development of a human adaptive immune system in cord blood cell-transplanted mice. *Science* **304**, 104-107 (2004).

27. Gimeno, R., *et al.* Monitoring the effect of gene silencing by RNA interference in human CD34+ cells injected into newborn RAG2-/- gammac-/- mice: functional inactivation of p53 in developing T cells. *Blood* **104**, 3886-3893 (2004).
28. Hombrink, P., *et al.* High-throughput identification of potential minor histocompatibility antigens by MHC tetramer-based screening: feasibility and limitations. *PLoS One* **6**, e22523 (2011).
29. Jorritsma, A., *et al.* Selecting highly affine and well-expressed TCRs for gene therapy of melanoma. *Blood* **110**, 3564-3572 (2007).
30. Hodis, E., *et al.* A landscape of driver mutations in melanoma. *Cell* **150**, 251-263 (2012).
31. Pleasance, E.D., *et al.* A small-cell lung cancer genome with complex signatures of tobacco exposure. *Nature* **463**, 184-190 (2010).
32. Wang, G.C., Dash, P., McCullers, J.A., Doherty, P.C. & Thomas, P.G. T Cell Receptor Diversity Inversely Correlates with Pathogen-Specific Antibody Levels in Human Cytomegalovirus Infection. *Science Translational Medicine* **4**, 128ra142 (2012).
33. Seitz, S., *et al.* Reconstitution of paired T cell receptor alpha- and beta-chains from microdissected single cells of human inflammatory tissues. *Proc Natl Acad Sci U S A* **103**, 12057-12062 (2006).
34. Matsushita, H., *et al.* Cancer exome analysis reveals a T-cell-dependent mechanism of cancer immunoediting. *Nature* **482**, 400-404 (2012).
35. Castle, J.C., *et al.* Exploiting the mutanome for tumor vaccination. *Cancer Res* **72**, 1081-1091 (2012).
36. van Rooij, N., *e t al.* Tumor exome analysis reveals neo-antigen-specific T cell reactivity in an Ipilimumab-responsive melanoma. *J Clin Oncol* (in the press).
37. de Witte, M.A., *et al.* An inducible caspase 9 safety switch can halt cell therapy-induced autoimmune disease. *J Immunol* **180**, 6365-6373 (2008).
38. Kieback, E., Charo, J., Sommermeyer, D., Blankenstein, T. & Uckert, W. A safeguard eliminates T cell receptor gene-modified autoreactive T cells after adoptive transfer. *Proc Natl Acad Sci U S A* **105**, 623-628 (2008).
39. Kalos, M., *et al.* T cells with chimeric antigen receptors have potent antitumor effects and can establish memory in patients with advanced Leukemia. *Sci Transl Med* **3**, 95ra73 (2011).
40. Kebriaei, P., *et al.* Infusing CD19-directed T cells to augment disease control in patients undergoing autologous hematopoietic stem-cell transplantation for advanced B-lymphoid malignancies. *Hum Gene Ther* **23**, 444-450 (2012).
41. Li, H. & Durbin, R. Fast and accurate short read alignment with Burrows-Wheeler transform. *Bioinformatics* **25**, 1754-1760 (2009).
42. Li, H., *et al.* The Sequence Alignment/Map format and SAMtools. *Bioinformatics* **25**, 2078-2079 (2009).
43. Krzywinski, M., *et al.* Circos: an information aesthetic for comparative genomics. *Genome Res* **19**, 1639-1645 (2009).

| SUPPLEMENTARY MATERIALS

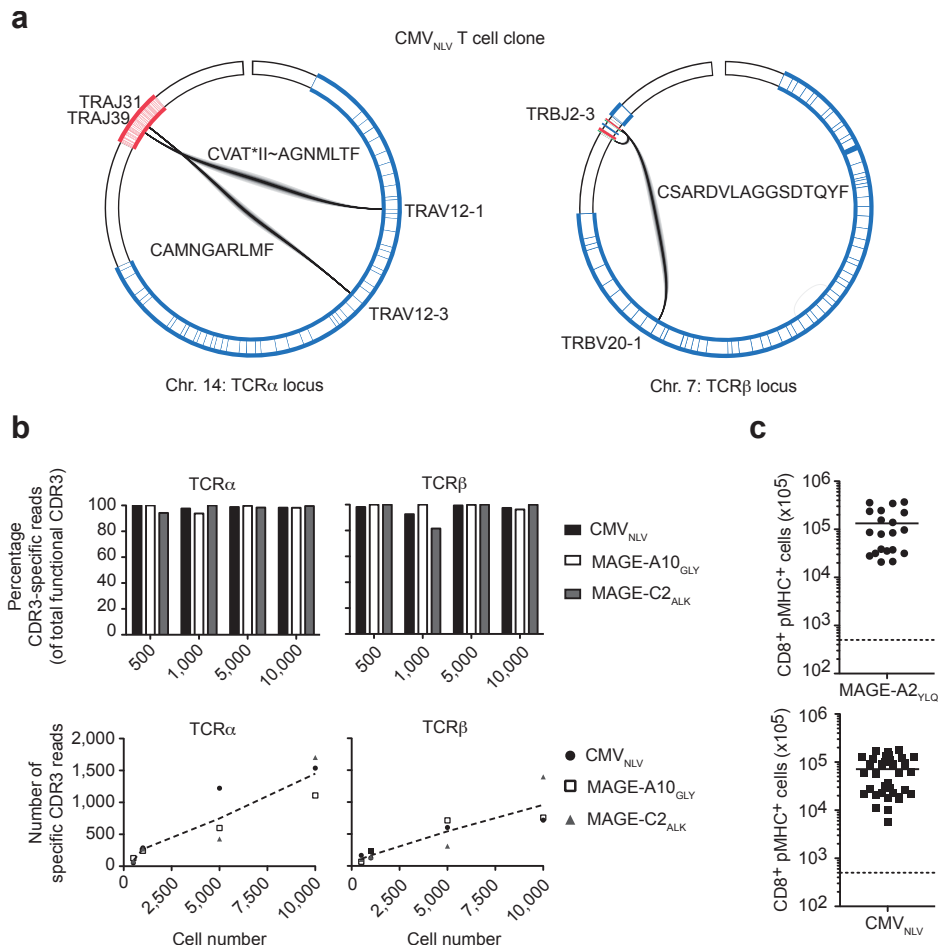

Supplementary Figure 1. Validation of the TCR gene capture method. (**a**) Circular plots representing chromosomal rearrangements identified in genomic DNA isolated from a CMV$_{NLV}$-specific T-cell clone. Blue lines represent chromosomal positions of TCR V-elements and red lines mark TCR J-elements. Identified TCR rearrangements are depicted by the lines connecting V- and J-elements. (**b**) Total read numbers and relative abundance of clonotypic CDR3 sequences after TCR gene capture with gDNA from indicated cell numbers of CMV$_{NLV}$, MAGE-A10$_{GLY}$ and MAGE-C2$_{ALK}$ specific T-cell clones. (**c**) Total number of live CD8$^+$, pMHC-multimer$^+$ cells 14 days after sort of single MAGE-A2$_{YLQ}$ and CMV$_{NLV}$ specific CD8$^+$ T-cells from PBMC. Dotted lines indicate the minimum number of cells required for reliable TCR gene capture.

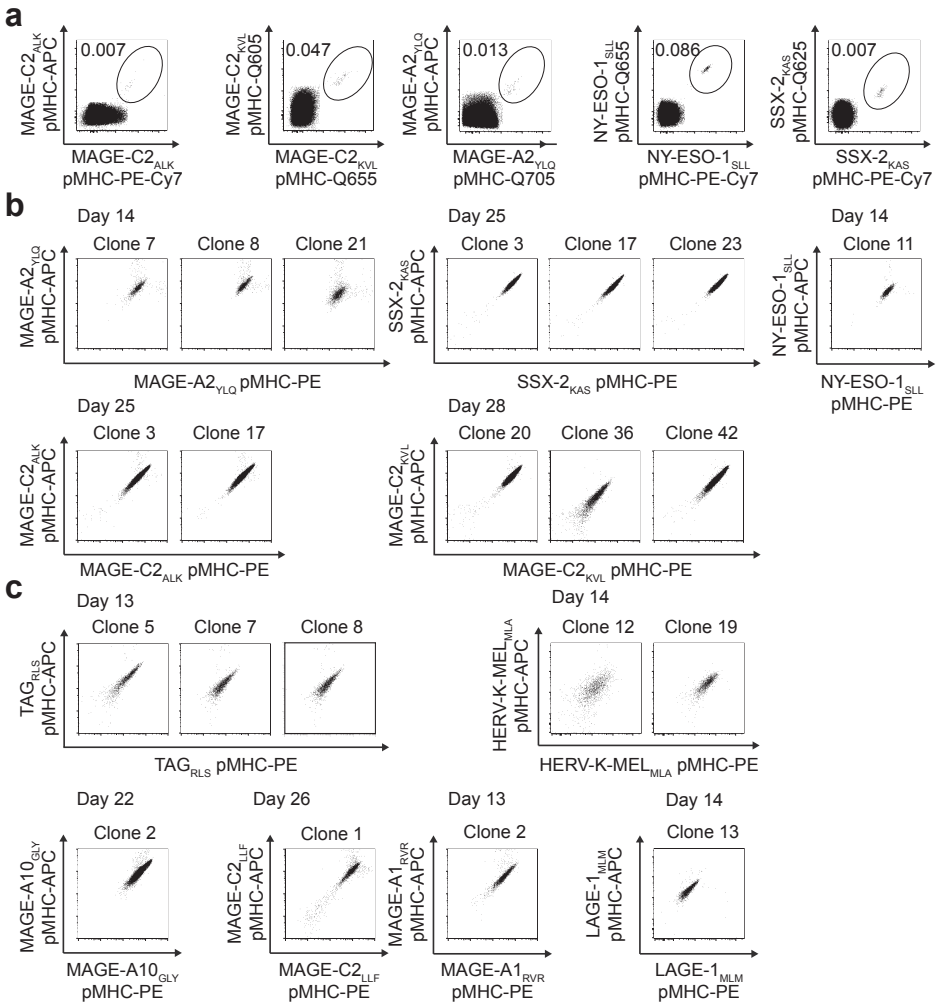

Supplementary Figure 2. Isolation of low-frequency Cancer/Germline (C/G)-antigen-specific T-cells from PBMC and TIL material for use in TCR gene capture. (**a**) Identification of CD8$^+$ T-cell responses specific for the MAGE-C2, MAGE-A2, NY-ESO-1 and SSX-2 C/G-antigens in peripheral blood material of melanoma patients by combinatorial coding analysis. Plots depict pMHC-multimer stains of live, CD8$^+$, 'Dump'-negative cells. (**b**) Flow cytometric analysis of clonal T-cell cultures specific for the MAGE-C2, MAGE-A2, NY-ESO-1 and SSX-2 C/G-antigens analyzed at indicated days after single cell-sorting from peripheral blood. Plots depict pMHC-multimer stains of live, CD8$^+$ cells. Representative plots out of >150 pMHC-multimer+ samples analyzed are shown. (**c**) Flow cytometric analysis of clonal T-cell cultures specific for the MAGE-A1, MAGE-A10, MAGE-C2, HERV-K-MEL, LAGE-1 and TAG C/G-antigens analyzed at indicated days after single cell-sorting from TIL material of melanoma-patients. Plots show pMHC-multimer stains of live, CD8$^+$ cells. Representative plots out of 82 pMHC-multimer$^+$ samples analyzed are shown.

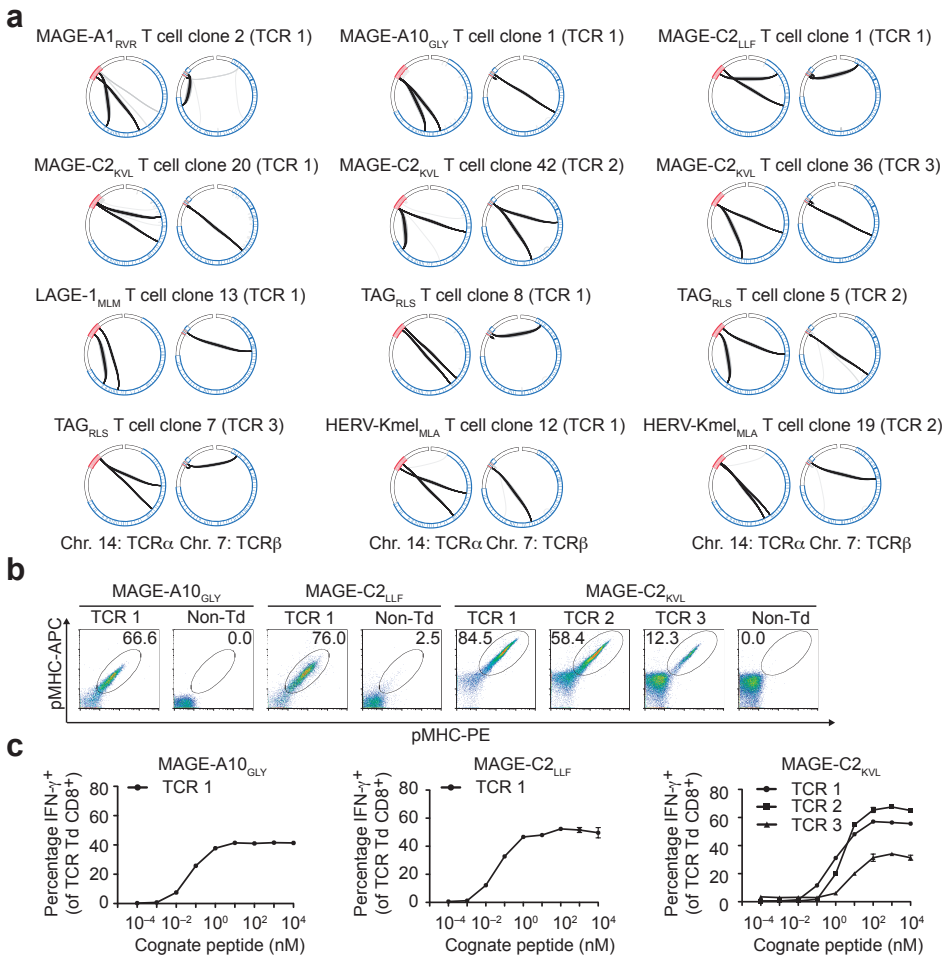

Supplementary Figure 3. Assembly of a Cancer/Germline (C/G)-antigen specific TCR library by TCR gene capture. (**a**) Circular plots representing chromosomal rearrangements identified in gDNA from MAGE-A1$_{RVR}$, MAGE-A10$_{GLY}$, MAGE-C2$_{LLF}$, MAGE-C2$_{KVL}$, HERV-Kmel$_{MLA}$, LAGE-1$_{MLM}$ and TAG$_{RLS}$ specific T-cells. Representative plots out of 59 samples analyzed are shown. Blue lines represent chromosomal positions of TCR V-elements and red lines mark TCR J-elements. Identified TCR rearrangements are depicted by the lines connecting V- and J-elements. (**b**) Validation of indicated TCRs by pMHC-multimer staining 13-15 days after retroviral transduction of primary human PBLs. Plots depict pMHC-multimer stains of live, CD8$^+$ T-cells. (**c**) Validation of functional activity of the indicated TCRs by analysis of IFN-γ production of TCR Td PBLs in response to peptide-loaded target cells 13-15 days after retroviral transduction. Data was normalized by correction of the percentage IFN-γ$^+$ CD8$^+$ T-cells by the percentage of TCR Td CD8$^+$ T-cells. Please note that chromosomal rearrangements only occurring with low frequency are not displayed in the circular plots for reasons of clarity.

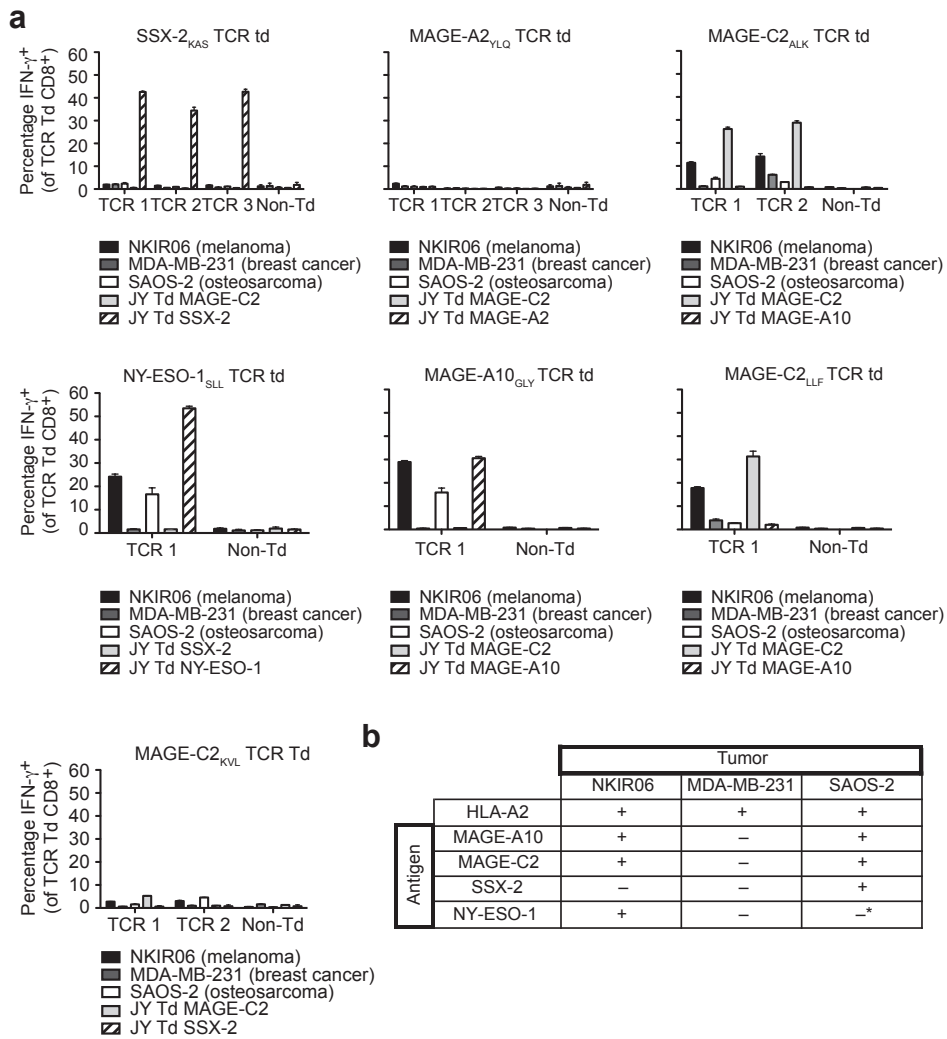

		Tumor		
		NKIR06	MDA-MB-231	SAOS-2
Antigen	HLA-A2	+	+	+
	MAGE-A10	+	–	+
	MAGE-C2	+	–	+
	SSX-2	–	–	+
	NY-ESO-1	+	–	–*

Supplementary Figure 4. Recognition of endogenously processed antigen by identified Cancer/Germline (C/G)-antigen specific TCRs. (**a**) IFN-γ production of TCR Td PBLs in response to indicated tumor cell lines and control cell lines engineered to express C/G-antigens, analyzed 12-13 days after retroviral transduction. Data was normalized by correction of the percentage IFN-γ^+ $CD8^+$ T-cells by the percentage of TCR Td $CD8^+$ T-cells. Note that MAGE-$C2_{KVL}$ TCR 3 Td T-cells displayed non-specific activity and were not analyzed further. (**b**) Expression of the indicated C/G-antigens within the tumor-cell lines used, as determined by real-time PCR. (*) SAOS-2 tumor cells do express LAGE-1 which contains a peptide sequence identical to the NY-ESO-$1_{157\text{-}165}$ T-cell epitope.

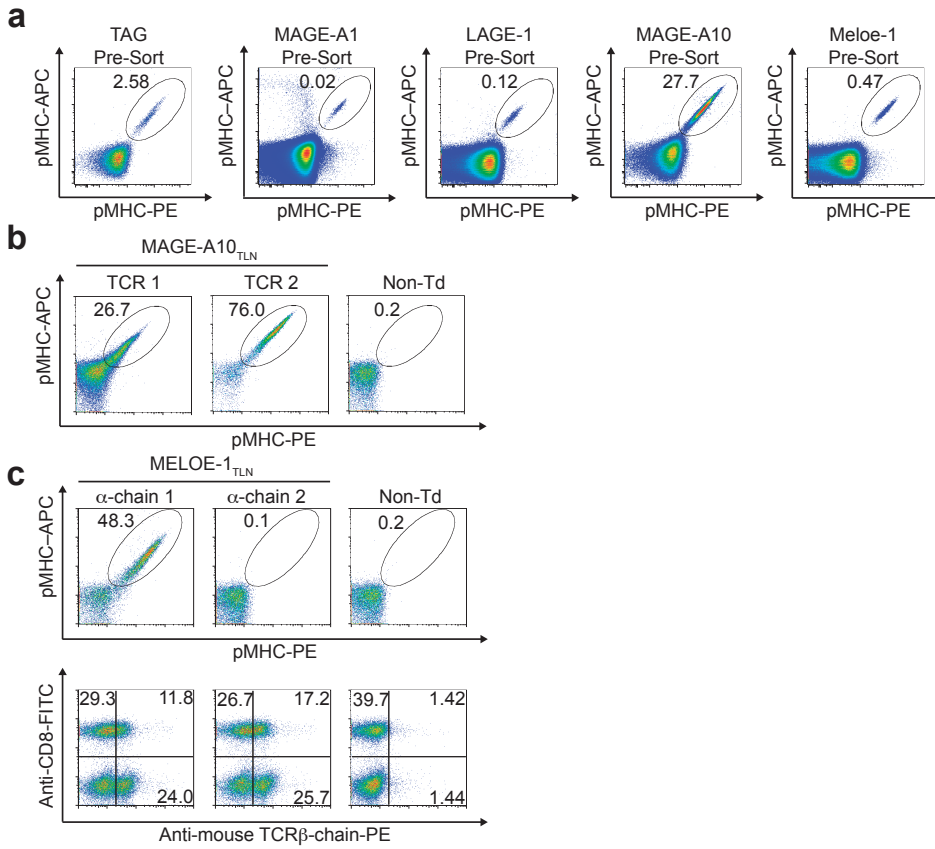

Supplementary Figure 5. Identification of tumor antigen-reactive TCRs in antigen-specific T-cell populations obtained from human tumor material by frequency-based matching. (**a**) Frequency of TAG_{RLS}, $MAGE\text{-}A1_{RVR}$ and $LAGE\text{-}1_{MLM}$ specific $CD8^+$ T-cells in TIL , and frequency of $MAGE\text{-}A10_{GLY}$ specific $CD8^+$ T-cells within a TIL-derived T-cell line, as measured by pMHC-multimer staining and flow cytometry prior to isolation. Plots show pMHC-multimer stains of live, CD8+ T-cells. (**b**) Validation of indicated $MAGE\text{-}A10_{GLY}$ specific TCRs by pMHC-multimer staining 12 days after retroviral transduction of primary human PBL. Plots depict pMHC-multimer stains of live, $CD8^+$ T-cells. (**c**) Validation of indicated $MELOE\text{-}1_{TLN}$ TCRs by pMHC-multimer staining 14 days after retroviral transduction of primary human PBL. Plots depict pMHC-multimer stains of live, $CD8^+$ T-cells and anti-mouse TCRβ chain constant domain stains of live cells, the latter as a control for successful transduction. Note that the pMP71-TCR-flex vector encodes the mouse TCR constant domains (Suppl. Fig. 11)

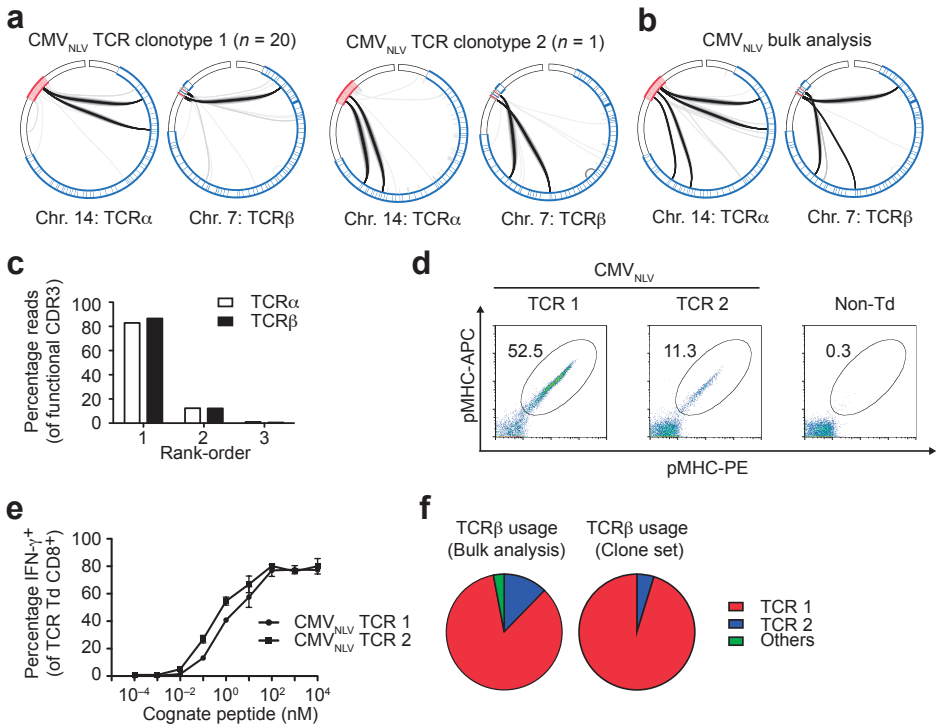

Supplementary Figure 6. TCR gene capture allows identification of TCRs from a CMV$_{NLV}$-specific T-cell population by frequency-based matching. CMV$_{NLV}$ specific CD8$^+$ T-cells were isolated from peripheral blood, either as single cells or as a bulk population, by pMHC-multimer based cell-sorting. TCR gene rearrangements were subsequently identified in expanded single cell clones, or within the bulk antigen-specific T-cell population by TCR gene capture. (**a**) Circular plots representing the two TCR clonotypes identified in gDNA from 21 CMV$_{NLV}$-specific CD8$^+$ T-cell clones analyzed 14 days after single-cell-sorting. (**b**) Circular plots representing the chromosomal rearrangements identified in gDNA isolated from 3 x 10^5 bulk-sorted CMV$_{NLV}$-specific CD8$^+$ T-cells. (**c**) Frequency-based matching of TCRα and TCRβ CDR3s according to their relative abundance among all functional CDR3s. (**d**) Flow cytometric analysis of CMV$_{NLV}$-TCR expression in primary human PBLs 13 days after retroviral transduction using pMHC-multimers. Plots show pMHC-multimer stain of live, CD8$^+$ T-cells. (**e**) Validation of functional activity of the indicated TCRs by analysis of IFN-γ production of CMV$_{NLV}$-TCR Td PBLs in response to peptide-loaded target cells 13 days after retroviral transduction. Data were normalized by correction of the percentage IFN-γ$^+$ CD8$^+$ T-cells by the percentage of TCR Td CD8$^+$ T-cells. (**f**) Comparison of the relative frequency of TCRβ CDR3s among sequenced CMV$_{NLV}$-specific T-cell clones and in the bulk CMV$_{NLV}$ specific T-cell population. Note that the correct CMV-specific TCRs that jointly make up >98% of the antigen-specific T-cell pool could be directly inferred from the analysis of bulk cells. Please note that chromosomal rearrangements only occurring with low frequency are not displayed in the circular plots for reasons of clarity.

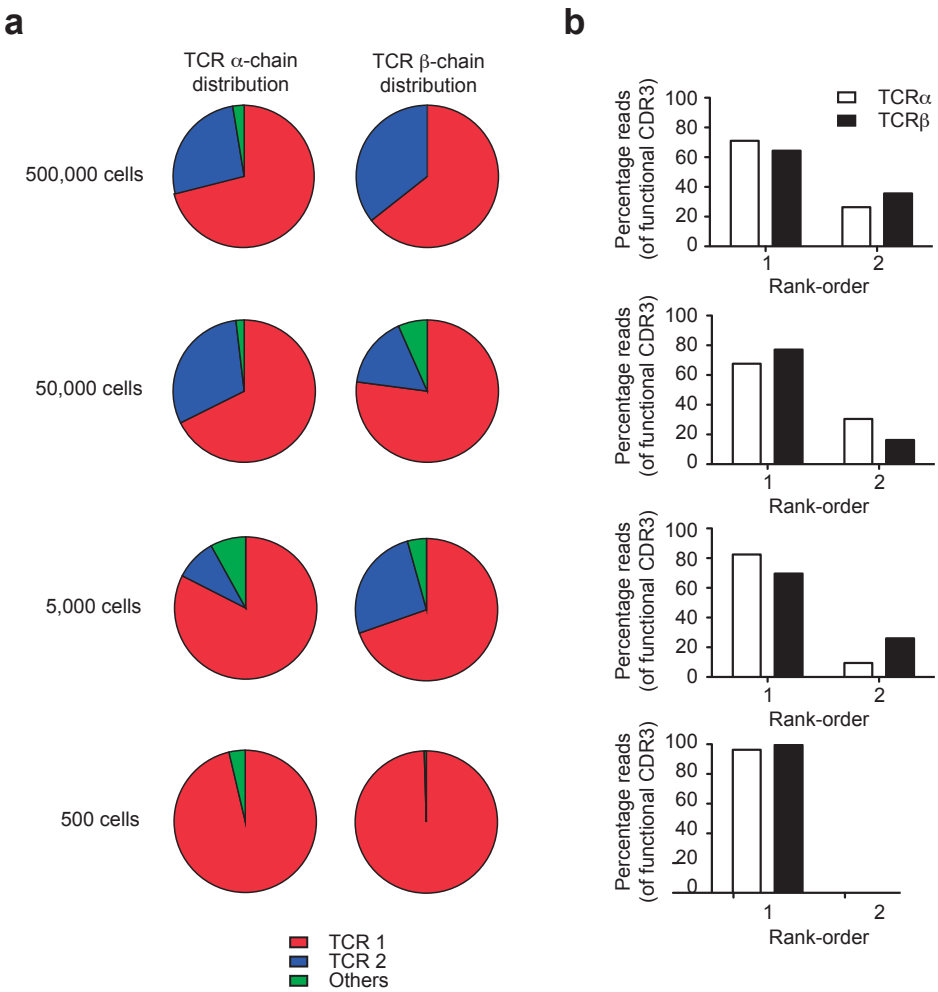

Supplementary Figure 7. Sensitivity of TCR gene capture in bulk T-cell populations. Indicated numbers of MAGE-A10$_{GLY}$ specific CD8$^+$ T-cells were obtained from a TIL-derived T-cell line by pMHC-multimer based cell-sorting and gDNA from these cell populations was subsequently analyzed by TCR gene capture. (**a**) Comparison of the relative frequency of TCRα and TCRβ CDR3s among all functional CDR3s identified by TCR gene capture from the indicated cell numbers. (**b**) Frequency-based matching of TCRα and TCRβ CDR3s according to their relative abundance among all functional CDR3s identified by TCR gene capture from the indicated cell numbers.

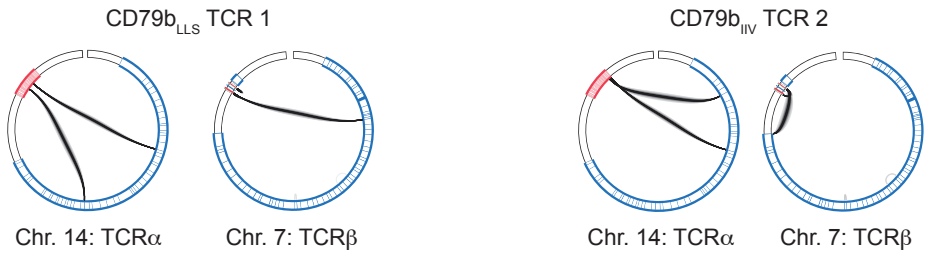

Supplementary Figure 8. Identification of allo-HLA-restricted TCRs specific for two HLA-A2 restricted epitopes of the CD79b lineage antigen. Allo-HLA-restricted CD8 T-cell populations were obtained by pMHC-multimer based enrichment of PBLs from an HLA-A2 negative individual and analyzed with TCR gene capture. Circular plots representing chromosomal rearrangements identified in gDNA from two CD79b-specific T-cell clones. Please note that chromosomal rearrangements only occurring with low frequency are not displayed in the circular plots for reasons of clarity.

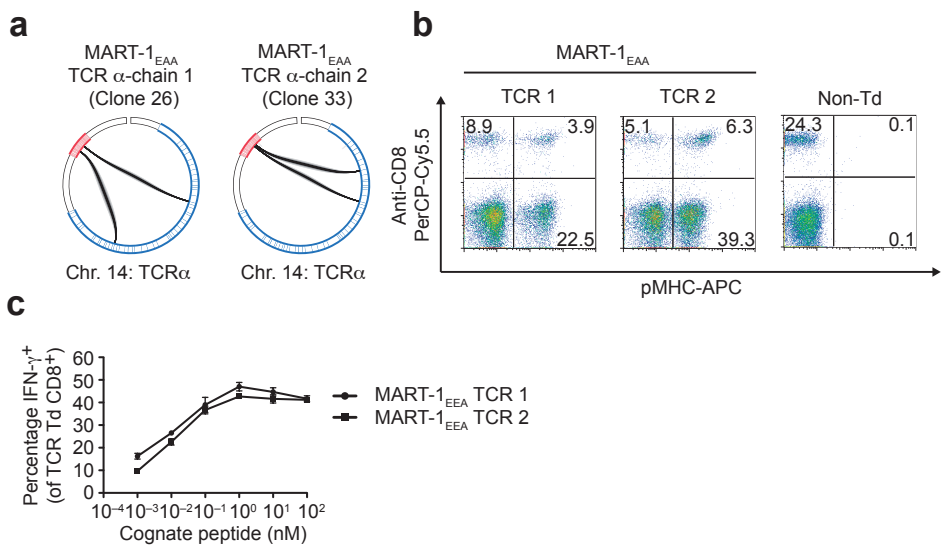

Supplementary Figure 9. Identification of MART-1 specific TCRs in T-cells from Balb/c Rag2$^{-/-}$ Il2rg$^{-/-}$ mice reconstituted with human hematopoietic progenitor cells (HIS-mice). Human hematopoietic progenitor cells were lentivirally modified with the MART-1 specific 1D3 TCRβ chain and used to reconstitute Balb/c Rag2$^{-/-}$ Il2rg$^{-/-}$ mice. Single splenic T-cells from reconstituted mice were sorted using MART-1 specific HLA-A2-multimers, expanded and used for TCR gene capture. (**a**) Circular plots representing chromosomal rearrangements identified in gDNA from two MART-1 specific T-cell clones. Representative plots out of 22 successfully analyzed samples are shown. (**b**) Validation of indicated TCRs by pMHC-multimer staining after retroviral transduction of primary human PBL. Plots depict pMHC-multimer stains of live, CD8$^+$ T-cells. (**c**) Validation of functional activity of the indicated TCRs by analysis of IFN-γ production of MART-1$_{EAA}$-TCR Td PBLs in response to peptide-loaded target cells after retroviral transduction. Data were normalized for TCR Td CD8$^+$ T-cells. Please note that chromosomal rearrangements only occurring with low frequency are not displayed in the circular plots for reasons of clarity.

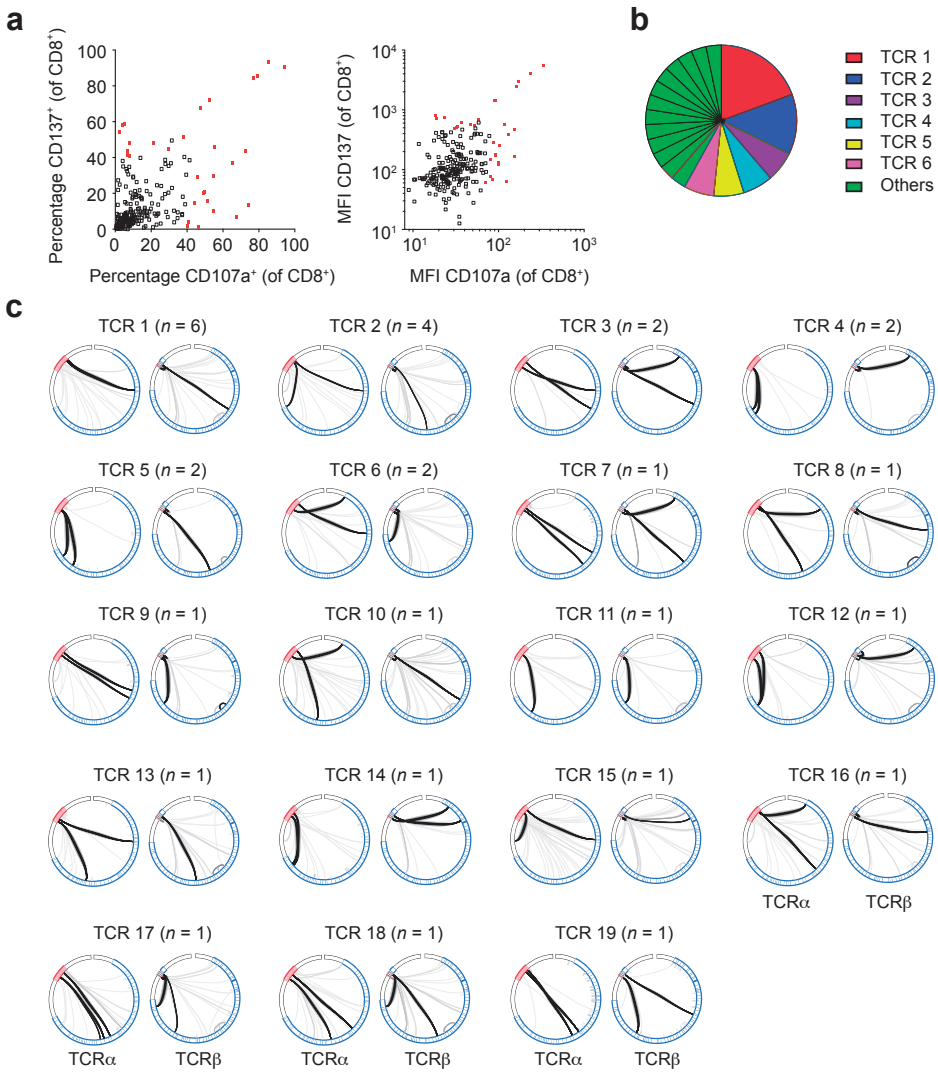

Supplementary Figure 10. Assembly of a patient-specific library of tumor-reactive TCRs without prior knowledge on antigen reactivity. Single CD8$^+$ T-cells were obtained from NKIR44 TIL and briefly expanded. (**a**) Subsequently, expression of CD107a and CD137 upon stimulation with autologous tumor was analyzed. 34 out of 234 T-cell clones (14.5%) showed apparent tumor-reactivity, as defined by the percentage of CD107a or CD137-positive cells and the MFI of CD107a and CD137 expression. 31 of these tumor reactive T-cell clones were analyzed by TCR gene capture (marked in red). (**b**) Frequency of 19 TCR clonotypes identified by TCR gene capture in the set of 31 tumor-reactive T-cell clones. (**c**) Circular plots representing the TCR clonotypes identified in gDNA from the 31 tumor-reactive T-cell clones. Please note that chromosomal rearrangements only occurring with low frequency are not displayed in the circular plots for reasons of clarity.

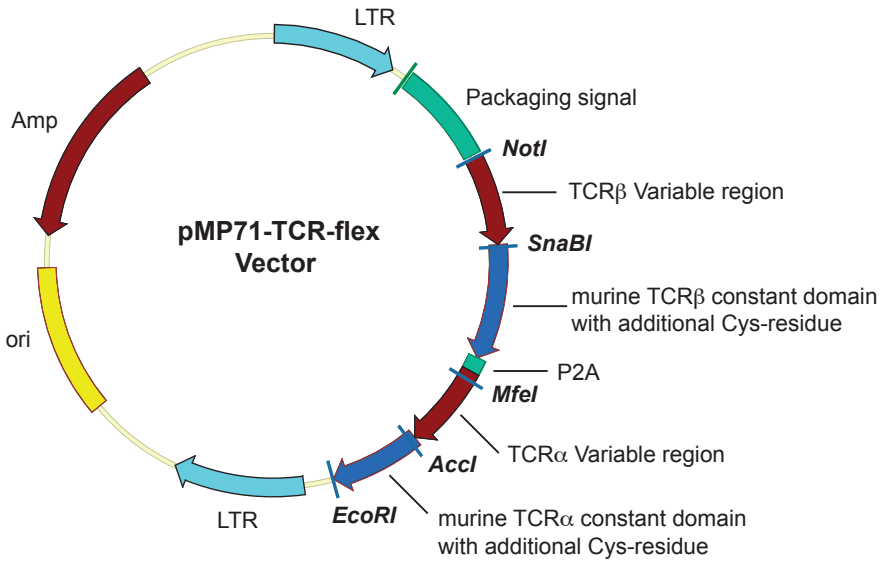

Supplementary Figure 11. pMP71-TCR-flex vector for rapid cloning of TCR sequences. Unique NotI/SnaBI and MfeI/AccI cut-sites allow the one-step exchange of variable TCR domains. To maximize TCR expression, the vector encodes codon-optimized murine TCRαβ constant domains with additional cysteine residues, and a porcine teschovirus-derived P2A sequence to link TCR chains in a β-2A-α configuration.

| SUPPLEMENTARY METHODS

Identification of tumor antigen-specific T-cells in patient material. PBMC and TIL material was obtained from individuals with stage IV melanoma following informed consent and in accordance with institutional, Dutch and Danish guidelines. PBMC material was prepared by Ficoll-Isopaque density centrifugation. TIL cells were isolated and expanded as previously described[1]. Patient samples were then used to screen for T-cells specific for any of 145 melanoma-associated antigens by pMHC-multimer combinatorial coding analyses as described[2,3]. All T-cell responses identified were confirmed in an independent analysis.

Flow cytometric sorting of bulk T-cell populations from human material. Cell-sorting was performed on a FACS Aria I (BD-Biosciences), MoFlo Legacy (Beckman Coulter) or MoFlo Astrios (Beckman Coulter). Bulk antigen-specific T-cell populations were obtained from either PBMC or TIL material by sorting of live, single $CD8^+$ T-cells stained with PE-/APC-labeled pMHC-multimers and an antibody against CD8 (BD-Biosciences; SK1; 1:50), combined with antibodies against CD3 (BD-Biosciences; SK7; 1:50) and CD4 (BD-Biosciences; SK3; 1:50) where applicable. For isolation of bulk tumor-reactive T-cell populations, 1×10^5 TIL were incubated with 1×10^5 autologous tumor cells for 16 hours, in the presence of a CD107a specific antibody (BD-Biosciences; H4A3; 1:100). Subsequently, cells were stained with antibodies against CD3 (BD-Biosciences; SK7; 1:50) and CD8 (BD-Biosciences SK1; 1:50) and, where indicated, with the IOTest Beta Mark Kit (Beckman Coulter).

Short-term T-cell expansion from human PBMC and TIL. Live, single $CD8^+$ T-cells were sorted from PBMC and TIL material using PE-/APC-labeled pMHC-multimers and an antibody against CD8 (BD-Biosciences; SK1; 1:50) to obtain $CD8^+$ T-cell populations with known antigen-reactivities. Live, single $CD8^+$ T-cells were sorted from TIL stained with antibodies against CD8 (BD-Biosciences; SK1; 1:50), CD3 (BD-Biosciences; SK7; 1:50) and CD4 (BD-Biosciences; SK3; 1:50) to obtain $CD8^+$ T-cell populations for which reactivity against autologous tumor could subsequently be tested.

In both cases, sorted single cells were collected in 96-well round-bottom culture plates containing 2×10^5 irradiated PBMC, 30 ng ml^{-1} CD3-specific antibody (OKT-3; Janssen-Cilag) and 3000 IU ml^{-1} rh-IL-2 (Novartis) in 200 µl X-VIVO medium (Lonza) supplemented with 10% (v/v) AB serum (Life Technologies), Penicillin/Streptomycin (Roche), GlutaMax (Life Technologies) and 50 µM 2-Mercaptoethanol (Sigma-Aldrich). After 7 days, 100 µl was replaced with fresh medium supplemented with rh-IL-2 (3000 IU ml^{-1} final). A confirmatory pMHC-multimer stain was used to identify positive $CD8^+$ T-cell clones by flow cytometry at day 14 (75% of all sorts yielded pMHC-multimer$^+$ T-cell clones). For identification of tumor-reactive $CD8^+$ T-cell populations, 25% of the resulting T-cell material was harvested and incubated with 5×10^4 autologous tumor cells for 16 hours, in the presence of a CD107a specific antibody (BD-Biosciences; H4A3; 1:100). For flow cytometric analysis, samples were stained with antibodies against CD3 (BD-Biosciences; SK7; 1:50), CD8 (BD-Biosciences; SK1; 1:50) and CD137 (BD-Biosciences; 4B4-1; 1:30).

Selected $CD8^+$ T-cell clones were generally used directly for TCR capture or in some cases further expanded using 30 ng ml^{-1} CD3-specific antibody (OKT-3; Janssen-Cilag) and 3000 IU ml^{-1} rh-IL-2 (Novartis) in supplemented X-VIVO media at a 1:200 T-cell: feeder cell ratio to allow capture at a later point in time.

Mice. All animal experiments were performed in accordance with institutional, Dutch and German guidelines and were approved by the Experimental Animal Committee of the Academic Medical Center of the University of Amsterdam (AMC) and by the Landesamt für Arbeitsschutz, Gesundheitsschutz und Technische Sicherheit, Berlin.

Balb/c *Rag2*$^{-/-}$ *Il2rg*$^{-/-}$ mice reconstituted with human $CD34^+CD38^-$ lineage-negative (CD3, CD11c, CD19, CD56, or BDCA2) hematopoietic progenitor cells ('HIS-mice') were generated as previously described[4]. Fetal tissue for reconstitution of mice was received following informed consent and with prior approval by the Medical Ethical Committee of the AMC Amsterdam. Lentiviral transductions of human hematopoietic progenitor cells were carried out as described[5] with a pHEF lentiviral vector modified to co-express mouse CD47, the P2A linked 1D3 TCRβ chain and GFP. T-cell populations from HIS mice were obtained by sort of live, single $CD8^+$ T-cells stained with PE-/APC-labeled pMHC-multimers, and sorted single cells were expanded as described previously[6,7].

Mice transgenic for human TCRαβ loci and a chimeric HLA-A2 gene[8] were vaccinated with 2 μg pCDNA-NY-ESO-1 vector and 2 μg GM-CSF by gene gun. 12 months later, mice were boosted by s.c. tail base injection of 100 μg NY-ESO-$1_{157\text{-}165}$ peptide and 50 μg CpG 1826 (Invivogen), diluted in 100 μl PBS, emulsified in an equal volume IFA (Sigma). At day 7 post-peptide vaccination, bulk T-cell populations of interest were obtained by sorting of cells stained with PE/APC-labeled NY-ESO-$1_{157\text{-}165}$-HLA-A2-k^b multimers and antibodies against CD3 (BioLegend; 17A2; 1:100) and CD8 (BioLegend; 53-6.7; 1:100).

Retroviral transduction and expression of T-cell receptors. For retrovirus production, FLYRD18 packaging cells were plated into 10 cm dishes at 1.2×10^6 cells per dish. After 24 hours, cells were transfected with 10 μg retroviral vector DNA using FuGENE 9 Transfection reagent (Roche Diagnostics and Promega). Human T-cell expander beads (Life Technologies) were used to select $CD3^+$ cells from PBMC material and activate 1.5×10^6 $CD3^+$ cells per 24-well with 100 IU ml^{-1} rh-IL-2 and 5 ng ml^{-1} rh-IL-15 (Peprotech). After 48 hours, $0.2–0.5\times10^6$ activated $CD3^+$ cells were resuspended in 0.5 ml harvested retroviral supernatant and 0.5 ml media supplemented with rh-IL-2 (100 IU ml^{-1} final) and rh-IL-15 (5 ng ml^{-1} final) and transferred to Retronectin (Takara)-coated plates. Plates were centrifuged for 90 minutes at 430 *g*. Transduction efficiency was determined at 72 hours, by pMHC-multimer and an antibody against mouse TCRβ chain (BD-Biosciences; H57-597; 1:100).

Cytokine-production assays. T2 cells were pulsed with the indicated peptides for 90 minutes at 37 °C and washed. For T-cell stimulation, 1×10^5 TCR-transduced PBMCs were incubated with 1×10^5 peptide-pulsed T2 cells or 1×10^5 tumor cells in the presence of 1 μl ml^{-1} Golgiplug (BD-Biosciences). After 5 hour incubation at 37°C, cells were washed and stained with antibodies against CD3 (BD-Biosciences; SK7; 1:50) and CD8 (BD-Biosciences; SK1; 1:50). Intracellular

levels of IFN-γ were determined by flow cytometry using the Cytofix/Cytoperm kit (BD-Biosciences) and an antibody against IFN-γ (BD-Biosciences; 25723; 1:50), according to the manufacturer's guidelines. The data was normalized by correction of percentage IFN-γ$^+$ CD8$^+$ T-cells with the frequency of TCR Td CD8$^+$ T-cells as measured by pMHC-multimer stain or with an antibody specific for the mouse TCRβ chain constant domain on the day of the assay.

C/G-antigen expression in tumor cell lines. Total RNA was isolated from tumor cell lines with RNeasy Mini Kit (Qiagen). cDNA was synthesized using Superscript II Reverse Transcriptase (Life Technologies) according to manufacturer's guidelines. Taqman probes specific for *SSX2* (SSX-2), *CTAG1B* (NY-ESO-1), *MAGEA10* (MAGE-A10) and *MAGEC2* (MAGE-C2) were obtained from Applied Biosystems. Real-time PCRs were performed using Taqman Universal PCR Master Mix (Applied Biosystems) according to manufacturer's guidelines on a 7500 Fast Real-Time PCR System (Applied Biosystems).

Nomenclature of C/G-antigens. The official gene names for the C/G-antigens analyzed in this study are: *CTAG2* (LAGE-1); *MAGEA1* (MAGE-A1); *MAGEA2* (MAGE-A2); *MAGEA10* (MAGE-A10); *MAGEC2* (MAGE-C2); *CTAG1B* (NY-ESO-1); *SSX2* (SSX-2) and *ERVK13-1* (HERV-K-MEL). Note that *ERVK13-1* is a human endogenous retroviral sequence with a C/G-antigen restricted expression pattern[9].

| REFERENCES

1. Friedman, K.M., *et al.* Tumor-specific CD4+ melanoma tumor-infiltrating lymphocytes. *J Immunother* 35, 400-408 (2012).
2. Andersen, R.S., *et al.* Dissection of T-cell antigen specificity in human melanoma. *Cancer Res* 72, 1642-1650 (2012).
3. Kvistborg, P., *et al.* TIL therapy broadens the tumor-reactive CD8(+) T cell compartment in melanoma patients. *OncoImmunology* 1, 409-418 (2012).
4. van Lent, A.U., *et al.* In vivo modulation of gene expression by lentiviral transduction in "human immune system" Rag2-/- gamma c -/- mice. *Methods Mol Biol* 595, 87-115 (2010).
5. Legrand, N., *et al.* Functional CD47/signal regulatory protein alpha (SIRP(alpha)) interaction is required for optimal human T- and natural killer- (NK) cell homeostasis in vivo. *Proc Natl Acad Sci U S A* 108, 13224-13229 (2011).
6. Yssel, H., De Vries, J.E., Koken, M., Van Blitterswijk, W. & Spits, H. Serum-free medium for generation and propagation of functional human cytotoxic and helper T cell clones. *J Immunol Methods* 72, 219-227 (1984).
7. Spits, H. & Yssel, H. Cloning of Human T and Natural Killer Cells. *Methods* 9, 416-421 (1996).
8. Li, L.P., *et al.* Transgenic mice with a diverse human T cell antigen receptor repertoire. *Nat Med* 16, 1029-1034 (2010).
9. Schiavetti, F., Thonnard, J., Colau, D., Boon, T. & Coulie, P.G. A human endogenous retroviral sequence encoding an antigen recognized on melanoma by cytolytic T lymphocytes. *Cancer Res* 62, 5510-5516 (2002).